Chapter 6
Overconstrained Mechanisms

By definition, an overconstrained mechanism is a mechanism for which Grübler's formula (4.1) yields a degree of freedom $F > 0$ only because the system of kinematic constraint equations has a sufficiently large defect $d > 0$. It is known that a simple closed kinematic chain with $n < 7$ joint variables has a degree of freedom $F > 0$ only if it is overconstrained. Sections 6.1 – 6.4 are devoted to simple closed chains with four, with five and with six revolute joints. In the remaining Sects. 6.5 – 6.11 other types of overconstrained mechanisms are analyzed.

The planar four-bar and the spherical four-bar with $n = 4$ revolute joints are among the oldest overconstrained mechanisms. Two simple overconstrained mechanisms with $n = 6$ revolute joints are shown in Figs. 6.1 and 6.2. In Fig. 6.1 the fixed frame, three shafts and the cross-shaped central bodies of two Hooke's joints are interconnected by two frame-fixed revolutes and by two more revolutes in each Hooke's joint. The mechanism shown in Fig. 6.2 was invented by Sarrus. Body 4 has the single degree of freedom of translation along the x-axis. The body is connected to the frame 1 by two dyads (bodies 2,3 and 5,6) each dyad having three parallel revolute joints

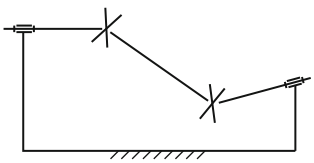

Fig. 6.1 Overconstrained mechanism composed of three shafts, two revolute and two Hooke's joints

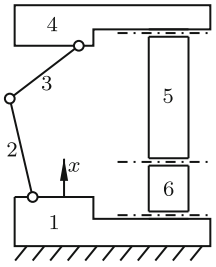

Fig. 6.2 Sarrus' overconstrained mechanism

© Springer-Verlag Berlin Heidelberg 2016

J. Wittenburg, *Kinematics*, DOI 10.1007/978-3-662-48487-6_6

perpendicular to the x-axis (otherwise arbitrarily directed, but not all six parallel).

6.1 Bricard's Theorem on Closed Chains with Revolute Joints

The early history of the search for overconstrained mechanisms was marked by chance discoveries and by ingenuity. The first systematic investigations were made by Delassus [15, 16]. An important step forward was made by Bricard's

Theorem 6.1. *In the case of $n = 6$ revolute joints the joint axes are, in every position of the system instantaneously, lines of a linear complex. In the case of $n = 5$ revolute joints the joint axes are, in every position of the system instantaneously, lines of a linear congruence. In the case of $n = 4$ revolute joints the joint axes are, in every position of the system instantaneously, generating lines of a ruled surface of order two (a quadric).*

Proof for the case $n = 6$ (Bricard [10]): Let joint i connect bodies i and $i-1$ $(i = 1, \ldots, 6$ cyclic), and let $\omega_i(\mathbf{n}_i, \mathbf{a}_i \times \mathbf{n}_i)$ be the associated velocity screw of body i relative to body $i-1$ (see (9.33)). The vectors $\mathbf{n}_i$ and $\mathbf{a}_i \times \mathbf{n}_i$ are the Plücker vectors of joint axis i. The velocity screw of body 6 relative to itself is zero. This is the set of equations

$$\sum_{i=1}^{6} \mathbf{a}_i \times \mathbf{n}_i \omega_i = \mathbf{0} \,, \qquad \sum_{i=1}^{6} \mathbf{n}_i \omega_i = \mathbf{0} \,. \tag{6.1}$$

Decomposition in some common reference frame yields six homogeneous linear equations with a (6×6)-coefficient matrix of vector coordinates multiplied by the column matrix of angular velocities. Since these latter ones are not all zero, the coefficient matrix must be singular. More precisely, some linear combination of its rows must be zero. In vector notation this is expressed by the six equations (one for each column of the matrix)

$$\mathbf{a} \cdot \mathbf{a}_i \times \mathbf{n}_i + \mathbf{b} \cdot \mathbf{n}_i = 0 \qquad (i = 1 \ldots, 6) \tag{6.2}$$

where $\mathbf{a}$ and $\mathbf{b}$ are vectors whose altogether six coordinates are the coefficients of the said linear combination. This is Eq.(2.25) defining the lines $(\mathbf{n}_i \,, \mathbf{a}_i \times \mathbf{n}_i)$ to be lines of the linear complex $(\mathbf{a}; \mathbf{b})$. End of proof.

Proof for the case $n = 5$: The closed kinematic chain with six axes is formally reduced to a chain with five axes if the sixth axis $(\mathbf{n}_6 \,, \mathbf{a}_6 \times \mathbf{n}_6)$ has *arbitrary* location while simultaneously $\omega_6 = 0$. Equations (6.1) lead again to (6.2). Because of the arbitrariness of $\mathbf{n}_6$ and $\mathbf{a}_6 \times \mathbf{n}_6$ the said linear complex $(\mathbf{a}; \mathbf{b})$ is now subject to a linear constraint equation. This proves

that the axes $1, \ldots, 5$ are lines of a linear congruence. The proof for the case $n = 4$ repeats the same arguments. With axes 5 and 6 being arbitrary the linear complex $(\mathbf{a}; \mathbf{b})$ is subject to two linear constraint equations. This ends the proof of the theorem.

The theorem states that (in the case $n = 6$, for example) a closed kinematic chain with six joint axes is *instantaneously* mobile if in the position under investigation the six joint axes are lines of a linear complex. Motion into another position is possible only if in every intermediate position the six joint axes are lines of a linear complex. In general, this is not the case if a single assembly position of a mechanism is the result of selecting at random six lines of a linear complex as joint axes. The theorem provides a new direction to the search for overconstrained systems, namely: Find closed kinematic chains having the property that its six axes belong in *every position* to a linear complex. This search led Bricard [10] to three classes of overconstrained mechanisms which are the subjects of Sects. 6.4.1, 6.4.2 and 6.4.3. The chapter begins with the celebrated Bennett mechanism which has four revolute joints.

6.2 Bennett Mechanism

In Sect. 5.4.1 the closed kinematical chain RCCC was investigated (see Fig. 5.3 and (5.43) – (5.51)). Bennett [8] noticed that the joint variables h_2, h_3 and h_4 in the three cylindrical joints are identically zero if the parameters satisfy the conditions

$$\left.\begin{array}{llll} \alpha_3 = \alpha_1\,, & \ell_3 = \ell_1\,, & \alpha_4 = \alpha_2\,, & \ell_4 = \ell_2\,, \\ \ell_2 \sin\alpha_1 = \ell_1 \sin\alpha_2\,, & h_1 = 0\,. & & \end{array}\right\} \tag{6.3}$$

A proof is given further below. With $h_2 = h_3 = h_4 \equiv 0$ all four joints of the mechanism are revolute joints with zero offset. This mechanism is called Bennett mechanism. It is an overconstrained mechanism with the degree of freedom $F = 1$. Grübler's formula (4.1) yields $F = -2+d$. Hence the number of dependent constraint equations is $d = 3$. According to Bricard's Theorem 6.1 the joint axes are, in every position of the mechanism instantaneously, generators of a hyperboloid.

From the condition $\ell_2 \sin\alpha_1 = \ell_1 \sin\alpha_2$ it follows that $\sin\alpha_1$ and $\sin\alpha_2$ have the same sign. Arbitrarily, the positive sign is assumed, i.e., angles in the interval $0 < \alpha_1, \alpha_2 < \pi$ (angles zero and π are excluded because only spatial mechanisms are investigated). The Bennett mechanism is specified by the three parameters ℓ_1, α_1 and α_2. Together they determine ℓ_2.
Note: The alternative decision to use as parameters the quantities ℓ_1, ℓ_2 and α_1 has the disadvantage that either no real angle α_2 or two different angles α_2 satisfy the condition $\ell_2 \sin\alpha_1 = \ell_1 \sin\alpha_2$. Two mechanisms differing in

α_2 only are not representing two types of Bennett mechanism, but simply two different Bennett mechanisms.

Kinematical properties of the Bennett mechanism are deduced from the equations governing the mechanism RCCC and from the conditions (6.3). First, it is proved that $h_2 = h_3 = h_4 \equiv 0$. Equation (5.51) reduces to $h_3 = 0$. This concludes the proof for h_3. From the symmetry of Eqs.(6.3) it follows that $h_2 \equiv 0$ if $h_4 \equiv 0$. The solution $h_4 \equiv 0$ requires that the numerator expression in (5.45) be identically zero. In addition, (5.43) is valid. Therefore, it must be shown that the equations

$$Ac_4 + Bs_4 - R = 0\,, \qquad Dc_4 + Es_4 + F = 0 \tag{6.4}$$

do not contradict each other. The coefficients A, B, R, D, E, F are those given in (5.44) and (5.46). In view of (6.3) they have the forms

$$\left.\begin{array}{lll} A = -S_1(S_1C_2c_1 + S_2C_1)\,, & B = S_1^2 s_1\,, & D = \ell_1(ac_1 + b)\,, \\ R = \quad S_1(S_2C_1c_1 + S_1C_2)\,, & E = -2\ell_1 S_1C_1 s_1\,, & F = \ell_1(bc_1 + a) \end{array}\right\} \tag{6.5}$$

with constants

$$a = S_1(2C_1C_2 - S_2^2)\,, \qquad b = S_2(2C_1^2 + C_1C_2 - 1)\,. \tag{6.6}$$

With these expressions Eqs.(6.4) are two linear equations for two unknowns:

$$S_1C_2\frac{1 + c_1c_4}{s_1s_4} + C_1S_2\frac{c_1 + c_4}{s_1s_4} = S_1\,, \qquad a\,\frac{1 + c_1c_4}{s_1s_4} + b\,\frac{c_1 + c_4}{s_1s_4} = 2S_1C_1\,. \tag{6.7}$$

The solution is

$$\frac{1 + c_1c_4}{s_1s_4} = \frac{1 - C_1C_2}{C_2 - C_1}\,, \qquad \frac{c_1 + c_4}{s_1s_4} = \frac{-S_1S_2}{C_2 - C_1}\,. \tag{6.8}$$

The difference of these two equations produces on the left-hand side the expression

$$\frac{(1 - c_1)(1 - c_4)}{s_1s_4} = \tan\frac{\varphi_1}{2}\tan\frac{\varphi_4}{2} \tag{6.9}$$

and on the right-hand side the constant

$$\frac{1 - (C_1C_2 - S_1S_2)}{C_2 - C_1} = \frac{1 - \cos(\alpha_1 + \alpha_2)}{2\sin\frac{\alpha_1+\alpha_2}{2}\,\sin\frac{\alpha_1-\alpha_2}{2}} = \frac{\sin\frac{\alpha_1+\alpha_2}{2}}{\sin\frac{\alpha_1-\alpha_2}{2}}\,. \tag{6.10}$$

It can have any positive or negative value. Thus, the result for φ_4 is

$$\tan\frac{\varphi_4}{2} = p\,\cot\frac{\varphi_1}{2}\,, \qquad p = \frac{\sin\frac{\alpha_1+\alpha_2}{2}}{\sin\frac{\alpha_1-\alpha_2}{2}}\,. \tag{6.11}$$

This equation relates to every angle $0 \le \varphi_1 \le 2\pi$ a single angle φ_4 (and vice versa) for which $h_4 \equiv 0$. This concludes the proof.

The existence of a single angle φ_4 for every angle φ_1 proves that the Bennett mechanism does not have a second configuration. Full-cycle rotatability in joint 1 follows also from the fact that in (6.4) $A^2 + B^2 - R^2 = (S_1 S_2 s_1)^2 \ge 0$ and $D^2 + E^2 - F^2 = [\ell_1 S_2 (C_1 + C_2) s_1]^2 \ge 0$.

Next, the relationship between φ_2 and φ_1 is established. For the mechanism RCCC it is given by Eqs.(5.48), (5.49). With (6.3) the coefficients A^*, B^*, R^* turn out to be the coefficients A, B, R in (6.5) with α_1 and α_2 interchanged. Because of (6.11) this means that $\varphi_2 = -\varphi_4$.

Finally, the relationship between φ_3 and φ_1 is established. Equation (5.50) reduces to $\cos\varphi_3 = \cos\varphi_1$. Hence either $\varphi_3 = \varphi_1$ or $\varphi_3 = -\varphi_1$. Another equation involving φ_3 is Eq.(5.53). With (6.3) it becomes

$$S_1 C_2 (c_3 + c_4) - S_2 (s_3 s_4 - C_1 c_3 c_4) + C_1 S_2 = 0 \,. \tag{6.12}$$

Depending on whether $\varphi_3 = \varphi_1$ or $\varphi_3 = -\varphi_1$ this is one of the two equations

$$S_1 C_2 (c_1 + c_4) - S_2 (\pm s_1 s_4 - C_1 c_1 c_4) + C_1 S_2 = 0 \,. \tag{6.13}$$

For $c_1 + c_4$ and for $c_1 c_4$ expressions obtained from (6.8) are substituted. It turns out that only the equation with the minus sign is identically satisfied. This shows that $\varphi_3 = -\varphi_1$.

Next, the angular velocity $\dot\varphi_4$ and the angular acceleration $\ddot\varphi_4$ are determined by differentiating (6.11) with respect to time. The first derivative yields

$$\dot\varphi_4 = -p\,\dot\varphi_1 \frac{\cos^2\frac{\varphi_4}{2}}{\sin^2\frac{\varphi_1}{2}} = -p\,\dot\varphi_1 \frac{1}{\sin^2\frac{\varphi_1}{2}(1 + \tan^2\frac{\varphi_4}{2})} \tag{6.14}$$

$$= -p\,\dot\varphi_1 \frac{1}{\sin^2\frac{\varphi_1}{2}(1 + p^2\cot^2\frac{\varphi_1}{2})} = -p\,\dot\varphi_1 \frac{1}{\sin^2\frac{\varphi_1}{2} + p^2\cos^2\frac{\varphi_1}{2}} \tag{6.15}$$

or, finally,

$$\dot\varphi_4 = -\dot\varphi_1 \frac{2p}{1 + p^2 - (1 - p^2)\cos\varphi_1} \,. \tag{6.16}$$

The ratio $\dot\varphi_4/\dot\varphi_1$ is oscillating 2π-periodically between the extremal values $-p$ and $-1/p$. Differentiating one more time yields for the angular acceleration the expression

$$\ddot\varphi_4 = -\ddot\varphi_1 \frac{2p}{1 + p^2 - (1 - p^2)\cos\varphi_1} + \dot\varphi_1^2 \frac{2p(1 - p^2)\sin\varphi_1}{[1 + p^2 - (1 - p^2)\cos\varphi_1]^2} \,. \tag{6.17}$$

Byshgens [13] and Dimentberg/Schor [18] gave the first proofs that the Bennett mechanism, the planar four-bar and the spherical four-bar are the

only overconstrained mechanisms composed of four links and four revolute joints. See also Dietmaier [19].

In Chap. 7 chains RR are investigated. A chain RR is a chain of three bodies interconnected by two revolute joints. One of the terminal bodies is the fixed frame. The other terminal body has the degree of freedom two. Subject of investigation are positions of the moving body and trajectories of body-fixed points. In the Bennett mechanism bodies 3 and 1 are the terminal bodies of two chains RR, one with joints 1, 2 on body 2 and the other with joints 3, 4 on body 4. Equations (6.3) and the relationships $\varphi_3 = -\varphi_1$, $\varphi_4 = -\varphi_2$ show that both chains RR are congruent. Every position of body 3 and the trajectories of all points of body 3 are generated by both chains RR. In Chap. 7 these statements are arrived at by arguments different from the ones used here.

6.3 Kinematical Chains with Five Revolute Joints

The only known 5R mechanism is the Goldberg mechanism treated in Sect. 6.3.1. Whether other types exist, is an unsettled question. If so, then the fifteen constant Denavit-Hartenberg parameters ℓ_i, α_i, h_i $(i = 1, \ldots, 5)$ satisfy certain conditions. A set of sufficient conditions is formulated as follows. The unit vectors in the polygon of vectors $\ell_i\mathbf{a}_i + h_i\mathbf{n}_i$ $(i = 1, \ldots, 5)$ are shown in Fig. 5.5a in which now all five joints are understood to be revolute joints. Woernle-Lee equations eliminate two joint variables. Five equations relating φ_3, φ_1, φ_5 are based on the products $\mathbf{n}_2 \cdot \mathbf{n}_4$, $\mathbf{n}_2 \cdot \mathbf{r}$, $\mathbf{n}_4 \cdot \mathbf{r}$, $\mathbf{r}^2$ and $\mathbf{r} \cdot \mathbf{n}_2 \times \mathbf{n}_4$ with the vector $\mathbf{r}$ pointing from $\mathbf{n}_2$ to $\mathbf{n}_4$. This vector has the two representations

$$\mathbf{r} = \begin{cases} h_2\mathbf{n}_2 + \ell_2\mathbf{a}_2 + h_3\mathbf{n}_3 + \ell_3\mathbf{a}_3 & \text{(right segment)} \\ -(h_4\mathbf{n}_4 + \ell_4\mathbf{a}_4 + h_5\mathbf{n}_5 + \ell_5\mathbf{a}_5 + h_1\mathbf{n}_1 + \ell_1\mathbf{a}_1) & \text{(left segment)}\,. \end{cases} \tag{6.18}$$

The fifth equation is the dual derivative of the first equation (see (3.50)). Evaluation of the equations by means of Table 5.2 is an elementary exercise left to the reader. The first equation is $\mathbf{n}_k \cdot \mathbf{n}_{k+2} = \mathbf{n}_k \cdot \mathbf{n}_{k-3}$ with $k = 2$. The equations are

$$\left.\begin{aligned} S_2S_3c_3 \quad\quad\quad\quad\quad\quad + A_1c_5 + B_1s_5 &= R_1\,, \\ \ell_3\,S_2s_3 + A_2c_5 + B_2s_5 &= R_2\,, \\ -h_2S_2S_3c_3 \quad + \ell_2\,S_3s_3 + A_3c_5 + B_3s_5 &= R_3\,, \\ \ell_2\,\ell_3\,c_3 + h_2\ell_3\,S_2s_3 + A_4c_5 + B_4s_5 &= R_4\,, \\ (\ell_2C_2S_3 + \ell_3S_2C_3)c_3 - h_3S_2S_3s_3 + A_5c_5 + B_5s_5 &= R_5\,. \end{aligned}\right\} \tag{6.19}$$

The coefficients of $c_3 = \cos\varphi_3$ and $s_3 = \sin\varphi_3$ are constants. The coefficients A_i, B_i, R_i $(i = 1, \ldots, 5)$ are abbreviations for linear functions of $c_1 = \cos\varphi_1$

and $s_1 = \sin\varphi_1$:

$$\left.\begin{aligned}
A_1 &= -S_4(S_1C_5c_1 + C_1S_5)\,, \qquad B_1 = S_4S_1s_1\,,\\
R_1 &= \;\; C_4(S_1S_5c_1 - C_1C_5) + C_2C_3\,,\\
A_2 &= -h_4S_4(S_1C_5c_1 + C_1S_5) + \ell_4S_1s_1\,,\\
B_2 &= \ell_4(S_1C_5c_1 + C_1S_5) + h_4S_4S_1s_1\,,\\
R_2 &= (h_4C_4 + h_5)(S_1S_5c_1 - C_1C_5) - (\ell_5S_1s_1 + h_1C_1 + h_2 + h_3C_2)\,,\\
A_3 &= S_4(\ell_1C_5s_1 - h_1S_5)\,, \qquad B_3 = S_4(\ell_1c_1 + \ell_5)\,,\\
R_3 &= -[C_4(\ell_1S_5s_1 + h_1C_5 + h_5) + C_3(h_2C_2 + h_3) + h_4]\,,\\
A_4 &= -\ell_4(\ell_1c_1 + \ell_5) - h_4S_4(\ell_1C_5s_1 - h_1S_5)\,,\\
B_4 &= -h_4S_4(\ell_1c_1 + \ell_5) + \ell_4(\ell_1C_5s_1 - h_1S_5)\,,\\
R_4 &= (h_4C_4 + h_5)(\ell_1S_5s_1 + h_1C_5) + \ell_1\ell_5c_1 + h_4h_5C_4 - h_2h_3C_2\\
&\quad + \tfrac{1}{2}[\ell_1^2 + \ell_4^2 + \ell_5^2 + h_1^2 + h_4^2 + h_5^2 - (\ell_2^2 + \ell_3^2 + h_2^2 + h_3^2)]\,,\\
A_5 &= h_5B_1 + A_1'\,, \qquad B_5 = -h_5A_1 + B_1' \qquad R_5 = R_1'
\end{aligned}\right\} \tag{6.20}$$

(A_1' , B_1' , R_1' are the dual derivatives of A_1 , B_1 , R_1 , respectively).
The first four Eqs.(6.19) are solved for c_3 , s_3 , c_5 , s_5 . In terms of coefficient determinants

$$c_3 = \frac{\Delta_{c3}}{\Delta}\,, \qquad s_3 = \frac{\Delta_{s3}}{\Delta}\,, \qquad c_5 = \frac{\Delta_{c5}}{\Delta}\,, \qquad s_5 = \frac{\Delta_{s5}}{\Delta}\,. \tag{6.21}$$

Δ_{c3} and Δ_{s3} are sums of products of three functions $A_iB_jR_k$, whereas Δ_{c5} , Δ_{s5} and Δ are sums of products of only two functions (B_jR_k or A_iR_k or A_iB_j). Substitution of (6.21) into the fifth Eq.(6.19) results after multiplication with Δ in an equation in which φ_1 is the only variable. This equation must be the identity equation. The highest-order terms are c_1^3 , $c_1^2s_1$, $c_1s_1^2$ and s_1^3 . In terms of the new variable $x_1 = \tan\varphi_1/2$ it is a 6th-order equation

$$a_6x_1^6 + a_5x_1^5 + \cdots + a_1x_1 + a_0 \equiv 0\,. \tag{6.22}$$

The coefficients are functions of the fifteen parameters. Without loss of generality, the parameter ℓ_1 can be set equal to one so that $\ell_2, \ldots, \ell_5$ and $h_1, \ldots, h_5$ are determined as multiples of ℓ_1 . Hence there are only fourteen essential parameters. Equations (6.19), (6.20) remain valid when the indices of all parameters and variables are cyclicly increased by 1 , by 2 , by 3 , by 4 . Hence altogether five 6th-order identity equations with variables $x_i = \tan\varphi_i/2$ $(i = 1, \ldots, 5)$ and with coefficients depending on the fourteen essential parameters are obtained. In each identity equation the seven coefficients must be zero. In addition, the conditions $c_3^2 + s_3^2 = 1$, $c_5^2 + s_5^2 = 1$ and four more such conditions must be satisfied. Hence altogether 45 functions of the parameters must be zero.

6.3.1 Goldberg Mechanism

Goldberg [20] recognized that an overconstrained 5R mechanism can be constructed by merging two Bennett mechanisms. Both mechanisms must be identical in the parameters α_1 and ℓ_1 and different in the third parameter, i.e., α_2 in one mechanism and $\alpha_3 \neq \alpha_2$ in the other (see Fig. 6.3a). The parameters satisfy Eqs.(6.3), i.e.,

$$\ell_2 = \ell_1 \frac{\sin\alpha_2}{\sin\alpha_1}\,, \qquad \ell_3 = \ell_1 \frac{\sin\alpha_3}{\sin\alpha_1} \tag{6.23}$$

as well as the identity of pairs of opposite bodies. All joints have zero offset. Four bodies have the parameters $\ell_1\,,\ \alpha_1$. In Fig. 6.3b the mechanisms are shown in positions in which they share body 1 with parameters $\ell_1\,,\ \alpha_1$. The degree of freedom two as well as the quantities ℓ_1 and α_1 remain unchanged when body 1 is removed while preserving all six joint axes (Fig. c). Indeed, none of the original Bennett mechanisms is mobile with other than the original quantities $\ell_1\,,\ \alpha_1$. In the system of Fig. 6.3d one of the two joints bridging both mechanisms is frozen in an arbitrarily chosen position β. This results in the Goldberg mechanism with five bodies and five revolute joints. It has five constant parameters, namely, the four essential parameters $\alpha_1\,,\ \alpha_2\,,\ \alpha_3\,,\ \beta$ and the length ℓ_1 which merely determines the size.

The bodies are newly labeled as shown in Fig. 6.3d. Body i is the body of length ℓ_i $(i = 1,\ldots,5)$. Joint 3 between bodies 2 and 3 is the mobile joint bridging the two Bennett mechanisms. Body 5 with joint axes 5 and 1 is the body created by freezing the joint in the position β. The coefficients $A_i\,,\ B_i\,,\ R_i$ $(i = 1,\ldots,5)$ in (6.19) and (6.20) depend on the parameters $\ell_5\,,\ \alpha_5$ of this body 5 and on the offsets $h_5\,,\ h_1$ of its joints 5 and 1. As preparatory step these four parameters are expressed in terms of β and of the parameters $\ell_2\,,\ \alpha_2$ and $\ell_3\,,\ \alpha_3$ of the two bodies merged into body 5. These two bodies are labeled body $2'$ and body $3'$, respectively. The vector $\mathbf{r}$ pointing from axis 5 to axis 1 has the two representations

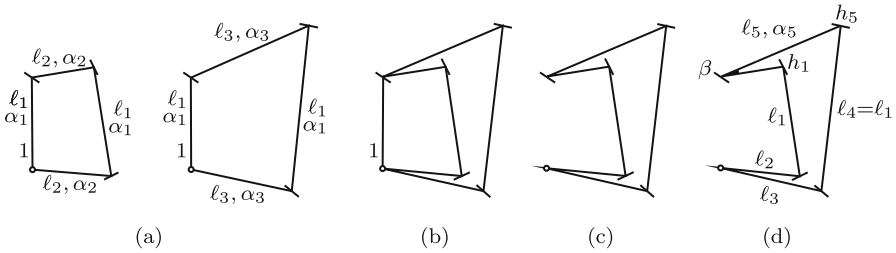

Fig. 6.3 Goldberg's creation of a 5R mechanism from two Bennett mechanisms

$$\mathbf{r} = \begin{cases} h_5\mathbf{n}_5 + \ell_5\mathbf{a}_5 + h_1\mathbf{n}_1 & \text{(right segment)} \\ \ell_2\mathbf{a}'_2 + \ell_3\mathbf{a}'_3 & \text{(left segment)} \end{cases} \tag{6.24}$$

with the notation familiar from Figs. 5.1 and 5.2. The unknown parameters are determined from five Woernle-Lee equations for the loop formed by the bodies $2'$, $3'$, 5 and by the joints 5, 1 and the frozen joint. The five equations are based on the scalar products $\mathbf{n}_5 \cdot \mathbf{n}_1$, $\mathbf{n}_5 \cdot \mathbf{r}$, $\mathbf{n}_1 \cdot \mathbf{r}$, $\mathbf{r}^2$ and $\mathbf{r} \cdot \mathbf{n}_5 \times \mathbf{n}_1$. The first four equations are obtained from Table 5.2:

$$\cos\alpha_5 = \cos\alpha_2 \cos\alpha_3 - \sin\alpha_2 \sin\alpha_3 \cos\beta \,, \tag{6.25}$$

$$h_5 + h_1 \cos\alpha_5 = \ell_2 \sin\alpha_3 \sin\beta = \ell_1 \frac{\sin\alpha_2 \sin\alpha_3 \sin\beta}{\sin\alpha_1} \,, \tag{6.26}$$

$$h_5 \cos\alpha_5 + h_1 = \ell_3 \sin\alpha_2 \sin\beta = \ell_1 \frac{\sin\alpha_2 \sin\alpha_3 \sin\beta}{\sin\alpha_1} \,, \tag{6.27}$$

$$\begin{aligned} h_5^2 + h_1^2 + 2h_5h_1 \cos\alpha_5 + \ell_5^2 &= \ell_2^2 + \ell_3^2 + 2\ell_2\ell_3 \cos\beta \\ &= \ell_1^2 \frac{\sin^2\alpha_2 + \sin^2\alpha_3 + 2\sin\alpha_2 \sin\alpha_3 \cos\beta}{\sin^2\alpha_1} \,. \end{aligned} \tag{6.28}$$

The fifth equation is the dual derivative of the first equation:

$$\begin{aligned} \ell_5 \sin\alpha_5 &= \ell_2 \sin\alpha_2 \cos\alpha_3 + \ell_3 \cos\alpha_2 \sin\alpha_3 \\ &\quad + (\ell_2 \cos\alpha_2 \sin\alpha_3 + \ell_3 \sin\alpha_2 \cos\alpha_3) \cos\beta \\ &= \ell_1 \frac{\sin^2\alpha_2 \cos\alpha_3 + \sin^2\alpha_3 \cos\alpha_2 + (\cos\alpha_2 + \cos\alpha_3) \sin\alpha_2 \sin\alpha_3 \cos\beta}{\sin\alpha_1} \,. \end{aligned} \tag{6.29}$$

From these equations the angle β is eliminated in order to express ℓ_5, h_1 and h_5 in terms of ℓ_1, α_2, α_3 and α_5 (Dietmaier [19]). Equation (6.29) with the expression for $\sin\alpha_2 \sin\alpha_3 \cos\beta$ from (6.25) yields

$$\ell_5 = \ell_1 \frac{(\cos\alpha_2 + \cos\alpha_3)}{\sin\alpha_1} \frac{(1 - \cos\alpha_5)}{\sin\alpha_5} = \ell_1 \frac{\cos\alpha_2 + \cos\alpha_3}{\sin\alpha_1} \tan\frac{\alpha_5}{2} \,. \tag{6.30}$$

The difference of (6.26) and (6.27) is

$$(h_5 - h_1)(1 - \cos\alpha_5) = 0 \,. \tag{6.31}$$

In the general case[1] $\alpha_5 \neq 0$, the equation yields $h_5 = h_1$. Equation (6.28) with ℓ_5 from (6.30) and with $\cos\beta$ from (6.25) yields

[1] Dietmaier investigates also the special cases $\alpha_5 = 0, \pi$ (axes 1 and 5 parallel). It is shown that $\alpha_5 = 0$ can occur only when the mechanism is a planar 2-d.o.f. mechanism. The case $\alpha_5 = \pi$ requires $\beta = 0$, $\alpha_2 + \alpha_3 = 0$ and $h_5 = h_1$ (arbitrary)

$$h_5 = h_1 = \ell_1 \, \frac{\sqrt{1 - \cos^2\alpha_2 - \cos^2\alpha_3 + 2\cos\alpha_2\cos\alpha_3\cos\alpha_5 - \cos^2\alpha_5}}{\sin\alpha_1(1+\cos\alpha_5)} \tag{6.32}$$

or with the identities

$$\left.\begin{aligned} &1 - \cos^2\alpha_2 - \cos^2\alpha_3 = \sin^2\alpha_2\sin^2\alpha_3 - \cos^2\alpha_2\cos^2\alpha_3 \\ &= -(\cos\alpha_2\cos\alpha_3 + \sin\alpha_2\sin\alpha_3)(\cos\alpha_2\cos\alpha_3 - \sin\alpha_2\sin\alpha_3) \\ &= -\cos(\alpha_2-\alpha_3)\cos(\alpha_2+\alpha_3)\ , \\ &2\cos\alpha_2\cos\alpha_3 = \cos(\alpha_2-\alpha_3) + \cos(\alpha_2+\alpha_3) \end{aligned}\right\} \tag{6.33}$$

$$h_5 = h_1 = \ell_1 \, \frac{\sqrt{[\cos(\alpha_2-\alpha_3) - \cos\alpha_5][\cos\alpha_5 - \cos(\alpha_2+\alpha_3)]}}{\sin\alpha_1(1+\cos\alpha_5)}\ . \tag{6.34}$$

Both ℓ_5 and h_5 are symmetric with respect to α_2 and α_3. The free parameters α_2, α_3 and α_5 are subject to the condition that h_5 must be real.

With ℓ_5 and $h_5 = h_1$ and with the parameters

$$h_2 = h_3 = h_4 = 0\ , \quad \ell_4 = \ell_1\ , \quad \alpha_4 = \alpha_1\ , \quad \ell_2 = \ell_1\frac{\sin\alpha_2}{\sin\alpha_1}\ , \quad \ell_3 = \ell_1\frac{\sin\alpha_3}{\sin\alpha_1} \tag{6.35}$$

the set of Eqs.(6.19), (6.20) and four more sets produced by cyclic permutation of all indices are formulated. In each set only the first four equations are used because the fifth equation is known to be satisfied if the first four are satisfied. Taking the first set, i.e., (6.19) and (6.20) as example three operations are carried out which are repeated with the other four sets of equations.

Operation 1: Introduction of the special parameters (6.35). The coefficients (6.20) are

$$\left.\begin{aligned} A_1 &= -S_1(S_1C_5c_1 + C_1S_5)\ , \qquad B_1 = S_1^2 s_1\ , \\ R_1 &= \ \ C_1(S_1S_5c_1 - C_1C_5) + C_2C_3\ , \\ A_2 &= \ell_1 S_1 s_1\ , \qquad B_2 = \ell_1(S_1C_5c_1 + C_1S_5)\ , \\ R_2 &= h_1[S_1S_5c_1 - C_1(1+C_5)] - \ell_5 S_1 s_1\ , \\ A_3 &= S_1(\ell_1C_5s_1 - h_1S_5)\ , \qquad B_3 = S_1(\ell_1c_1 + \ell_5)\ , \\ R_3 &= -C_1[\ell_1S_5s_1 + h_1(1+C_5)]\ , \\ A_4 &= -\ell_1(\ell_1c_1 + \ell_5)\ , \qquad B_4 = \ell_1(\ell_1C_5s_1 - h_1S_5)\ , \\ R_4 &= h_1(\ell_1S_5s_1 + h_1C_5) + \ell_1\ell_5c_1 + \tfrac{1}{2}[2\ell_1^2 + \ell_5^2 + 2h_1^2 - (\ell_2^2+\ell_3^2)]\ . \end{aligned}\right\} \tag{6.36}$$

Operation 2: From the first two Eqs.(6.19) it follows that

$$\cos\varphi_3 = \frac{R_1 - A_1c_5 - B_1s_5}{S_2S_3}\ , \qquad \sin\varphi_3 = \frac{R_2 - A_2c_5 - B_2s_5}{\ell_2S_2}\ . \tag{6.37}$$

Operation 3: Linear combinations of the equations result in two equations from which c_3 and s_3 are eliminated (note Eqs.(6.35) for h_2, ℓ_2 and ℓ_3):

$$\left.\begin{array}{rr} (\ell_1^2 A_1 - S_1^2 A_4)c_5 + & (\ell_1^2 B_1 - S_1^2 B_4)s_5 = \ell_1^2 R_1 - S_1^2 R_4 \ , \\ (A_2 - A_3)c_5 + & (B_2 - B_3)s_5 = R_2 - R_3 \ . \end{array}\right\} \tag{6.38}$$

Let in each set of four equations produced from (6.19), (6.20) by cyclic permutation of indices φ_j be the independent variable. Then the other two variables are φ_{j+2} and φ_{j-1} where φ_{j+2} is the variable associated with constant coefficients. Repetition of the same three operations result in Eqs.(6.37) of the general form

$$\left.\begin{array}{l} \cos\varphi_{j+2} = f(\varphi_j, \varphi_{j-1}) \ , \\ \sin\varphi_{j+2} = g(\varphi_j, \varphi_{j-1}) \end{array}\right\} (j = 1, 2, 3, 4, 5 \text{ cyclic}) \tag{6.39}$$

and in Eqs.(6.38) of the general form

$$\left.\begin{array}{l} u_1(\varphi_j)\cos\varphi_{j-1} + v_1(\varphi_j)\sin\varphi_{j-1} = w_1(\varphi_j) \ , \\ u_2(\varphi_j)\cos\varphi_{j-1} + v_2(\varphi_j)\sin\varphi_{j-1} = w_2(\varphi_j) \end{array}\right\} (j = 1, 2, 3, 4, 5) \ . \tag{6.40}$$

For a given angle φ_j each of these Eqs.(6.40) has two solutions φ_{j-1}. About the number of solutions common to both equations the following statement can be made. In the Goldberg mechanism two Bennett mechanisms are connected by joint 3. A single variable in a Bennett mechanism uniquely determines all other variables in the same Bennett mechanism. Hence a single common solution exists if φ_j is not φ_3. This solution is

$$\cos\varphi_{j-1} = \frac{w_1 v_2 - w_2 v_1}{u_1 v_2 - u_2 v_1} \ , \qquad \sin\varphi_{j-1} = \frac{u_1 w_2 - u_2 w_1}{u_1 v_2 - u_2 v_1} \ . \tag{6.41}$$

The associated angle φ_{j+2} is determined from (6.39).

In the case $\varphi_j = \varphi_3$ (6.19) and (6.20) are the equations

$$\left.\begin{array}{rrr} S_1 S_5 c_5 & + A_1^* c_2 + B_1^* s_2 = R_1^* \ , \\ \ell_5\, S_1 s_5 & + A_2^* c_2 + B_2^* s_2 = R_2^* \ , \\ \ell_1\, S_5 s_5 & + A_3^* c_2 + B_3^* s_2 = R_3^* \ , \\ \ell_1\, \ell_5\, c_5 & + A_4^* c_2 + B_4^* s_2 = R_4^* \end{array}\right\} \tag{6.42}$$

with the coefficients

$$\left.\begin{aligned}
A_1^* &= -S_1(C_2S_3c_3 + S_2C_3)\,, \qquad B_1^* = S_1S_3s_3\,,\\
R_1^* &= \quad C_1(S_2S_3c_3 - C_2C_3 + C_5)\,,\\
A_2^* &= \ell_1\Big[S_3s_3 - \frac{h_1}{\ell_1}\,S_1(C_2S_3c_3 + S_2C_3)\Big]\,,\\
B_2^* &= \ell_1\Big(C_2S_3c_3 + S_2C_3 + \frac{h_1}{\ell_1}\,S_1S_3s_3\Big)\,,\\
R_2^* &= \frac{\ell_1}{S_1}\Big[\frac{h_1}{\ell_1}\,S_1C_1(S_2S_3c_3 - C_2C_3 - 1) - S_2S_3s_3\Big]\,,\\
A_3^* &= \ell_1C_2S_3s_3\,, \qquad B_3^* = \ell_1(S_3c_3 + S_2)\,,\\
R_3^* &= -\frac{\ell_1}{S_1}\Big[C_1S_2S_3s_3 + \frac{h_1}{\ell_1}\,S_1(1 + C_5)\Big]\,,\\
A_4^* &= -\frac{\ell_1^2}{S_1}\Big[S_2 + S_3\Big(c_3 + \frac{h_1}{\ell_1}\,S_1C_2s_3\Big)\Big]\,,\\
B_4^* &= \frac{\ell_1^2}{S_1}\Big[C_2S_3s_3 - \frac{h_1}{\ell_1}\,S_1(S_3c_3 + S_2)\Big]\,,\\
R_4^* &= \frac{\ell_1^2}{S_1^2}\Big[S_2S_3\Big(\frac{h_1}{\ell_1}\,S_1C_1s_3 + c_3\Big) + 1 + C_2C_3 - \frac{(C_2 + C_3)^2}{1 + C_5}\Big]\,.
\end{aligned}\right\} \tag{6.43}$$

Equations (6.40) are

$$\left.\begin{aligned}
(\ell_1\ell_5A_1^* - S_1S_5A_4^*)c_2 + (\ell_1\ell_5B_1^* - S_1S_5B_4^*)s_2 &= \ell_1\ell_5R_1^* - S_1S_5R_4^*\,,\\
(\ell_1S_5A_2^* - \ell_5S_1A_3^*)c_2 + (\ell_1S_5B_2^* - \ell_5S_1B_3^*)s_2 &= \ell_1S_5R_2^* - \ell_5S_1R_3^*\,.
\end{aligned}\right\} \tag{6.44}$$

These two equations are identical, i.e., one of them is, independent of the variable φ_3, a constant multiple of the other. This is proved by verifying the identities

$$\left.\begin{aligned}
&(\ell_1\ell_5A_1^* - S_1S_5A_4^*)(\ell_1S_5B_2^* - \ell_5S_1B_3^*)\\
-\,&(\ell_1\ell_5B_1^* - S_1S_5B_4^*)(\ell_1S_5A_2^* - \ell_5S_1A_3^*) \equiv 0\,,\\
&(\ell_1\ell_5A_1^* - S_1S_5A_4^*)(\ell_1S_5R_2^* - \ell_5S_1R_3^*)\\
-\,&(\ell_1\ell_5R_1^* - S_1S_5R_4^*)(\ell_1S_5A_2^* - \ell_5S_1A_3^*) \equiv 0\,.
\end{aligned}\right\} \tag{6.45}$$

Each of them has, with different sets of constant coefficients, the form $p_1c_3^2 + p_2c_3s_3 + p_3c_3 + p_4s_3 + p_5 \equiv 0$. It is left to the reader to verify that in each of them $p_1 = p_2 = p_3 = p_4 = p_5 = 0$. Some of these proofs make use of the relationships

$$\left.\begin{aligned}
\frac{\ell_5^2}{\ell_1^2}\,S_1^2 &= \quad \frac{1 - C_5}{1 + C_5}\,(C_2 + C_3)^2\,, \qquad \frac{\ell_5}{\ell_1}\,S_1S_5 = (1 - C_5)(C_2 + C_3)\,,\\
S_5^2\Big(1 + \frac{h_1^2}{\ell_1^2}\,S_1^2\Big) &= -\frac{1 - C_5}{1 + C_5}\,(C_2 + C_3)^2 + 2(1 - C_5)(1 + C_2C_3)\,.
\end{aligned}\right\} \tag{6.46}$$

From the identity of the Eqs.(6.44) it follows that for a given angle φ_3 two sets of solutions φ_{1_k}, φ_{2_k}, φ_{4_k}, φ_{5_k} $(k = 1, 2)$ exist. For every solution φ_{2_k} $(k = 1, 2)$ the first two Eqs.(6.42) determine φ_{5_k}. Next, with $\varphi_j = \varphi_{2_k}$ (6.41) determines φ_{1_k}, and (6.39) determines φ_{4_k}. This concludes the analysis of the Goldberg mechanism.

It is unknown whether there exist 5R mechanisms other than Goldberg mechanisms. It was shown that its fourteen essential parameters must satisfy 45 conditions. Starting from the same[2] Eqs.(6.19), (6.20) Dietmaier [19] formulated a different set of 45 conditions $f_k = 0$ $(k = 1, \ldots, 45)$. A numerical search was made for zero-value minima of the function $F = \sum_{k=1}^{45} f_k^2$. Starting from a randomly picked point in the 14-dimensional parameter space the algorithm yields a certain minimum. If this minimum is not zero-valued, a new search is made with a new starting point. Among the zero-valued minima found only those are of interest which represent a new type of mechanism, i.e., neither a Goldberg mechanism nor a degenerate mechanism (planar, for example). Although Dietmaier tried 2×10^6 randomly picked starting points no new type of mechanism was found. This is not a proof, but a strong argument for the Goldberg mechanism to be the only 5R mechanism.

6.4 Kinematical Chains with Six Revolute Joints

The number of different types of overconstrained kinematic chains with six links and six revolute joints is unknown as well. Many different types are known. Simple examples are shown in Figs. 6.1 and 6.2. Systematic descriptions and analyses see in Baker [4, 7], Mavroidis/Roth [25, 26, 27] and Dietmaier [19]. Bricard [10] discovered three classes of mechanisms known as line-symmetric, plane-symmetric and trihedral mechanisms. They are the subjects of the three sections to come. Several other types of mechanisms are obtained by merging a number of Bennett mechanisms or of Goldberg mechanisms in the spirit of Goldberg's construction of the five-joint mechanism in Fig. 6.3 (Mudrov [29], Goldberg [20], Wohlhart [31, 32]). Dietmaier [19] found a new class of mechanisms by the numerical search described above. For six-link mechanisms the function to be investigated has the form $F = \sum_{k=1}^{102} f_k^2$ with functions f_k depending on eighteen Denavit-Hartenberg parameters. Dietmaier's mechanism is the subject of Sect. 6.4.4.

6.4.1 Line-Symmetric Bricard Mechanism

A mechanism having six arbitrarily skew, consecutively labeled joint axes 1, 2, 3, 4, 5, 6 is said to be symmetric with respect to a line z if the geometry is invariant to a 180°-rotation about this line. Bricard [10] recognized that such a mechanism is deformable with degree of freedom one, and that the symmetry is maintained in the course of deformation. His proof of mobility

[2] (6.19), (6.20) and Dietmaier's Eqs.(3-7) – (3-11) are identical if in the latter ones $(s_i, \theta_i, \alpha_i, a_i)$ is replaced by $(h_i, \varphi_i, \alpha_{i-1}, \ell_{i-1})$

one is as follows. Suppose that body 2 is fixed in some reference frame, and that the constraints in all joints are removed. Relative to the reference frame the line z is specified by four parameters, and the positions of bodies 1 and 3 are specified by additional twelve parameters. Through these altogether $N = 16$ parameters the positions of the other three bodies 4 , 5 and 6 are specified as well because of the symmetry with respect to z . Each revolute joint introduces five constraints. Because of the pairwise symmetry of joints the total number of independent constraints is only $3 \times 5 = 15$. The difference $N - 15 = 1$ is the degree of freedom of the mechanism. End of proof.

The line-symmetry of the mechanism finds its expression in the identities

$$\alpha_{i+3} = \alpha_i \ , \quad \ell_{i+3} = \ell_i \ , \quad \varphi_{i+3} \equiv \varphi_i \ , \quad h_{i+3} = h_i \quad (i = 1, 2, 3) \ . \tag{6.47}$$

In Fig. 6.4 the spatial polygon of vectors $h_i \mathbf{n}_i$ and $\ell_i \mathbf{a}_i$ $(i = 1, \ldots, 6)$ with these symmetrically distributed Denavit-Hartenberg parameters is shown schematically in projection along the line z . The angle φ_1 is chosen as independent variable. The angles φ_2 and φ_3 are the only dependent variables. The vector $\mathbf{r}$ joining the axes $\mathbf{n}_6$ and $\mathbf{n}_3$ has in the right and in the left segment the forms

$$\mathbf{r} = \begin{cases} \ell_3 \mathbf{a}_6 + h_1 \mathbf{n}_1 + \ell_1 \mathbf{a}_1 + h_2 \mathbf{n}_2 + \ell_2 \mathbf{a}_2 + h_3 \mathbf{n}_3 & \text{(right segment)} \\ -(\ell_3 \mathbf{a}_3 + h_1 \mathbf{n}_4 + \ell_1 \mathbf{a}_4 + h_2 \mathbf{n}_5 + \ell_2 \mathbf{a}_5 + h_3 \mathbf{n}_6) & \text{(left segment)} \ . \end{cases} \tag{6.48}$$

The Woernle-Lee equation $F_3^{\ell} = F_3^{r}$ with $F_3 = \mathbf{n}_6 \cdot \mathbf{r}$ is an equation involving only φ_1 and φ_2 . It is written in the form

$$\mathbf{n}_k \cdot \Big[\ell_3(\mathbf{a}_k + \mathbf{a}_{k-3}) + h_1(\mathbf{n}_{k+1} + \mathbf{n}_{k-2}) + \ell_1(\mathbf{a}_{k+1} + \mathbf{a}_{k-2}) \\ + h_2(\mathbf{n}_{k+2} + \mathbf{n}_{k-1}) + \ell_2(\mathbf{a}_{k+2} + \mathbf{a}_{k-1}) + h_3(\mathbf{n}_{k+3} + \mathbf{n}_k) \Big] = 0 \quad (k = 6) \ . \tag{6.49}$$

Copying coordinates from Table 5.2 and using (6.47) results in the equation

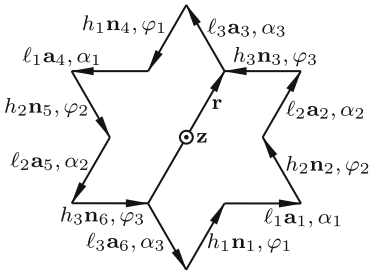

Fig. 6.4 Spatial polygon of vectors $h_i \mathbf{n}_i$ and $\ell_i \mathbf{a}_i$ of a Bricard mechanism with line of symmetry z . Vector $\mathbf{r}$ joining axes $\mathbf{n}_6$ and $\mathbf{n}_3$

$$\left.\begin{aligned}
&A_2\cos\varphi_2 + B_2\sin\varphi_2 = R_2\\
&A_2 = -h_3C_1S_2S_3\cos\varphi_1 + (\ell_2S_3 + \ell_3C_1S_2)\sin\varphi_1 - S_1S_2(h_1 + h_3C_3)\ ,\\
&B_2 = (\ell_2C_1S_3 + \ell_3S_2)\cos\varphi_1 + h_3S_2S_3\sin\varphi_1 + \ell_1S_2 + \ell_2S_1C_3\ ,\\
&R_2 = S_1S_3(h_2 + h_3C_2)\cos\varphi_1 - (\ell_1S_3 + \ell_3S_1C_2)\sin\varphi_1\\
&\qquad -h_1(C_1C_2 + C_3) - h_2(C_1C_3 + C_2) - h_3(1 + C_1C_2C_3)\ .
\end{aligned}\right\} \tag{6.50}$$

In the same way an equation for φ_3 as function of φ_1 is obtained on the basis of $F_3 = \mathbf{n}_5 \cdot \mathbf{r}$ with a vector $\mathbf{r}$ joining the axes $\mathbf{n}_5$ and $\mathbf{n}_2$. Equation (6.49) is replaced by

$$\begin{aligned}
&\mathbf{n}_k \cdot \Big[\ell_2(\mathbf{a}_k + \mathbf{a}_{k-3}) + h_3(\mathbf{n}_{k+1} + \mathbf{n}_{k-2}) + \ell_3(\mathbf{a}_{k+1} + a_{k-2})\\
&+h_1(\mathbf{n}_{k+2} + \mathbf{n}_{k-1}) + \ell_1(\mathbf{a}_{k+2} + \mathbf{a}_{k-1}) + h_2(\mathbf{n}_{k+3} + \mathbf{n}_k)\Big] = 0 \quad (k = 5)\ .
\end{aligned} \tag{6.51}$$

Evaluation results in the equation

$$\left.\begin{aligned}
&A_3\cos\varphi_3 + B_3\sin\varphi_3 = R_3\\
&A_3 = -h_2S_1S_2C_3\cos\varphi_1 + (\ell_1S_2C_3 + \ell_2S_1)\sin\varphi_1 - S_2S_3(h_1 + h_2C_1)\ ,\\
&B_3 = (\ell_1S_2 + \ell_2S_1C_3)\cos\varphi_1 + h_2S_1S_2\sin\varphi_1 + \ell_2C_1S_3 + \ell_3S_2\ ,\\
&R_3 = S_1S_3(h_2C_2 + h_3)\cos\varphi_1 - (\ell_1C_2S_3 + \ell_3S_1)\sin\varphi_1\\
&\qquad -h_1(C_1 + C_2C_3) - h_2(1 + C_1C_2C_3) - h_3(C_2 + C_1C_3)\ .
\end{aligned}\right\} \tag{6.52}$$

Each of the Eqs.(6.50) and (6.52) has two solutions $(\varphi_{2_1}, \varphi_{2_2})$ and $(\varphi_{3_1}, \varphi_{3_2})$, respectively. Their cosines and sines are

$$\left.\begin{aligned}
c_{j_k} &= \frac{A_jR_j + (-1)^kB_j\sqrt{A_j^2 + B_j^2 - R_j^2}}{A_j^2 + B_j^2}\ ,\\
s_{j_k} &= \frac{B_jR_j - (-1)^kA_j\sqrt{A_j^2 + B_j^2 - R_j^2}}{A_j^2 + B_j^2}
\end{aligned}\right\} \quad (j = 2,\,3\ ;\ k = 1,\,2)\ . \tag{6.53}$$

The square roots are identical:

$$\begin{aligned}
A_2^2 + B_2^2 - R_2^2 - (A_3^2 + B_3^2 - R_3^2) = \Big[&\ell_2^2(S_3^2 - S_1^2) + 2\ell_2S_2(\ell_3S_3C_1 - \ell_1S_1C_3)\\
&+ S_2^2(\ell_3^2 + h_3^2S_3^2 - \ell_1^2 - h_2^2S_1^2)\Big](\cos^2\varphi_1 + \sin^2\varphi_1 - 1) \equiv 0\ .
\end{aligned} \tag{6.54}$$

In order to determine which of the two solutions φ_2 belongs to which of the two solutions φ_3 an equation relating φ_2 and φ_3 is formulated by repeating the procedure once more with $F_3 = \mathbf{n}_4 \cdot \mathbf{r}$ and with a vector $\mathbf{r}$ joining the axes $\mathbf{n}_4$ and $\mathbf{n}_1$. Equation (6.49) is replaced by

$$\begin{aligned}
&\mathbf{n}_k \cdot \Big[\ell_1(\mathbf{a}_k + \mathbf{a}_{k-3}) + h_2(\mathbf{n}_{k+1} + \mathbf{n}_{k-2}) + \ell_2(\mathbf{a}_{k+1} + a_{k-2})\\
&+h_3(\mathbf{n}_{k+2} + \mathbf{n}_{k-1}) + \ell_3(\mathbf{a}_{k+2} + \mathbf{a}_{k-1}) + h_1(\mathbf{n}_{k+3} + \mathbf{n}_k)\Big] = 0 \quad (k = 4)\ .
\end{aligned} \tag{6.55}$$

Evaluation results in the equation

$$\left.\begin{aligned} &A_4\cos\varphi_3 + B_4\sin\varphi_3 = R_4 \\ &A_4 = -h_1S_1C_2S_3\cos\varphi_2 + (\ell_1C_2S_3 + \ell_3S_1)\sin\varphi_2 - S_2S_3(h_1C_1 + h_2)\ , \\ &B_4 = (\ell_1S_3 + \ell_3S_1C_2)\cos\varphi_2 + h_1S_1S_3\sin\varphi_2 + \ell_2S_3 + \ell_3C_1S_2\ , \\ &R_4 = S_1S_2(h_1C_3 + h_3)\cos\varphi_2 - (\ell_1S_2C_3 + \ell_2S_1)\sin\varphi_2 \\ &\qquad -h_1(1 + C_1C_2C_3) - h_2(C_1 + C_2C_3) - h_3(C_1C_2 + C_3)\ . \end{aligned}\right\} \tag{6.56}$$

In the example below it is shown that this equation is satisfied by the combinations $(\varphi_{2_1}, \varphi_{3_2})$ and $(\varphi_{2_2}, \varphi_{3_1})$.

Example: In Sect. 4.2.5 the special line-symmetric mechanism with parameters $\alpha_1 = \alpha_2 = \alpha_3 = \pi/2$, $\ell_1 = \ell_2 = \ell_3 = 0$ and $h_1 = h_2 = h_3 = 1$ was analyzed. With these parameters (6.50), (6.52) and (6.56) are, in this order,

$$c_2 - s_1s_2 = 1 - c_1\ , \qquad c_3 - s_1s_3 = 1 - c_1\ , \qquad c_3 - s_2s_3 = 1 - c_2\ . \tag{6.57}$$

Except for a difference in the definition of φ_1 the first equation is identical with (4.35), and the correlation between the solutions φ_2 and φ_3 has the form (4.38). Equations (6.53) are

$$\left.\begin{aligned} c_{2_{1,2}} = c_{3_{1,2}} &= \frac{1 - c_1 \pm s_1\sqrt{1 + 2c_1(1 - c_1)}}{1 + s_1^2}\ , \\ s_{2_{1,2}} = s_{3_{1,2}} &= \frac{-s_1(1 - c_1) \pm \sqrt{1 + 2c_1(1 - c_1)}}{1 + s_1^2}\ . \end{aligned}\right\} \tag{6.58}$$

By substituting these expressions it is verified that the third Eq.(6.57) is satisfied by the combinations $(\varphi_{2_1}, \varphi_{3_2})$ and $(\varphi_{2_2}, \varphi_{3_1})$. End of example.

According to Theorem 6.1 the six joint axes are, in every position of the mechanism instantaneously, lines of a linear complex. Conjecture: The axis of this linear complex intersects the line of symmetry z orthogonally. The following proof is due to Hon-Cheung [22]. It makes use of two properties of reciprocal polars which were established in Sect. 2.7.5 :
(a) The two transversals of any four independent complex lines are reciprocal polars of the linear complex.
(b) The common perpendicular of two reciprocal polars intersects orthogonally the axis of the linear complex.

Joint axes 1, 2, 3, 4 are line-symmetric to joint axes 4, 5, 6, 1 , respectively. According to (a) the two transversals of the former four axes are reciprocal polars and so are the two transversals of the latter four axes. The common perpendicular p of the former two reciprocal polars is line-symmetric to the common perpendicular p′ of the latter two reciprocal polars whence it follows that the common perpendicular of p and p′ intersects the line of symmetry z orthogonally. But according to (b) the axis of the linear complex intersects both p and p′ orthogonally, too. Therefore, this axis

and the common perpendicular of p and p′ intersecting z orthogonally are identical. End of proof.

6.4.2 Plane-Symmetric Bricard Mechanism

Another family of overconstrained mechanisms identified by Bricard [10] is referred to as plane-symmetric because of the pairwise symmetry of joint axes with respect to a plane Σ. In Fig. 6.5 the spatial polygon of vectors $h_i\mathbf{n}_i$ and $\ell_i\mathbf{a}_i$ $(i = 1, \ldots, 6)$ is shown schematically. The symmetry requires the opposite joint axes 1 and 4 to lie in Σ and to have zero offset: $h_1 = h_4 = 0$. It is left to the reader to verify that the remaining Denavit-Hartenberg parameters satisfy the conditions (for definitions see Fig. 5.1)

$$\left.\begin{array}{ll} \ell_6 = \ell_1 \,, & h_6 = h_2 \,, \\ \ell_5 = \ell_2 \,, & h_5 = h_3 \,, \\ \ell_4 = \ell_3 \,, & \end{array}\right\} \tag{6.59}$$

$$\left.\begin{array}{ll} \alpha_6 = \pi - \alpha_1 \,, & \varphi_6 \equiv -\varphi_2 \,, \\ \alpha_5 = -\alpha_2 \,, & \varphi_5 \equiv -\varphi_3 \,, \\ \alpha_4 = \pi - \alpha_3 \,. & \end{array}\right\} \tag{6.60}$$

Dissection of joints 1 and 4 produces two symmetrical twin halves of the system. Consider the twin half consisting of bodies 1, 2 and 3 and imagine body 2 to be fixed. Let body 1 be rotated relative to body 2 through an arbitrary *fixed* angle φ_2 so that joint axis 1 assumes a certain position. Likewise, let body 3 be rotated relative to body 2 through the angle φ_3 (*variable*) so that joint axis 4 generates an hyperboloid of revolution (in the case $\alpha_3 = 0$ a cylinder of radius ℓ_3 and in the case $\alpha_3 = \pi/2$ a plane every point of which outside a circle of radius ℓ_3 is located on two generators associated with different angles φ_3). The fixed axis 1 intersects

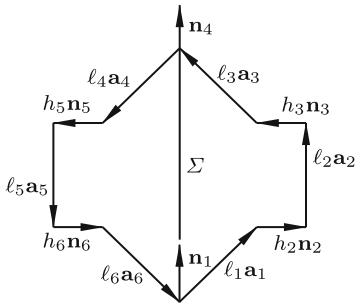

Fig. 6.5 Spatial polygon of vectors $h_i\mathbf{n}_i$ and $\ell_i\mathbf{a}_i$ of a Bricard mechanism symmetric with respect to plane Σ: $\ell_6 = \ell_1$, $h_6 = h_2$, $\ell_5 = \ell_2$, $h_5 = h_3$, $\ell_4 = \ell_3$

two generators of the hyperboloid (of the cylinder, of the plane in the said special cases) which are axes 4 coplanar with axis 1. Thus, for every φ_2 there are two angles φ_3 putting the twin half into a position with coplanar axes 1 and 4. The other twin half is mounted symmetrically thereby determining φ_1 and φ_4. Thus, not only mobility one of the mechanism is proved, but also the existence of two positions for a given independent angle φ_2. An equation relating φ_2 and φ_3 is derived from the intersection condition of the axes 1 and 4. This condition is written in the form (see Fig. 6.5)

$$\lambda\mathbf{n}_1 + \ell_1\mathbf{a}_1 + h_2\mathbf{n}_2 + \ell_2\mathbf{a}_2 + h_3\mathbf{n}_3 + \ell_3\mathbf{a}_3 + \mu\mathbf{n}_4 = \mathbf{0} \tag{6.61}$$

with unknowns λ and μ of dimension length. Decomposition of the vectors results in three equations relating λ, μ, φ_2 and φ_3. Vector coordinates are copied from Table 5.2. The simplest equations are obtained by decomposition on body 3, i.e., by evaluating the equation

$$\lambda\mathbf{n}_{k-2} + \ell_1\mathbf{a}_{k-2} + h_2\mathbf{n}_{k-1} + \ell_2\mathbf{a}_{k-1} + h_3\mathbf{n}_k + \ell_3\mathbf{a}_k + \mu\mathbf{n}_{k+1} = \mathbf{0} \tag{6.62}$$

with $k = 3$. This results in the set of equations

$$\left.\begin{aligned}
&\lambda(C_1C_2 - S_1S_2c_2) + \mu C_3 + \ell_1 s_2 S_2 + h_2 C_2 + h_3 &&= 0\,,\\
&\lambda[C_1S_2s_3 + S_1(s_2c_3 + c_2s_3C_2)] + \ell_1(c_2c_3 - s_2s_3C_2) + h_2S_2s_3 + \ell_2c_3 + \ell_3 &&= 0\,,\\
&\lambda[C_1S_2c_3 - S_1(s_2s_3 - c_2c_3C_2)] - \mu S_3 - \ell_1(c_2s_3 + s_2c_3C_2) + h_2S_2c_3 - \ell_2s_3 &&= 0\,.
\end{aligned}\right\} \tag{6.63}$$

The first two equations are solved for λ and μ. Substitution into the third equation and simple ordering of terms results in the desired equation relating φ_2 and φ_3 (terms c_2^2 and s_2^2 occuring in this process have identical coefficients; the same is true for c_3^2 and s_3^2)

$$A\cos\varphi_3 + B\sin\varphi_3 = R \tag{6.64}$$

with coefficients

$$\left.\begin{aligned}
A &= (-\ell_1C_1C_2S_3 + \ell_2S_1S_2S_3 - \ell_3S_1C_2C_3)\cos\varphi_2\\
&\quad + S_1S_3(h_2C_2 + h_3)\sin\varphi_2 + \ell_1S_1S_2S_3 - \ell_2C_1C_2S_3 - \ell_3C_1S_2C_3\,,\\
B &= S_1S_3(h_2 + h_3C_2)\cos\varphi_2 + (\ell_1C_1S_3 + \ell_3S_1C_3)\sin\varphi_2 + h_3C_1S_2S_3\,,\\
R &= (\ell_1C_1S_2C_3 + \ell_2S_1C_2C_3 - \ell_3S_1S_2S_3)\cos\varphi_2 - h_2S_1S_2C_3\sin\varphi_2\\
&\quad + \ell_1S_1C_2C_3 + \ell_2C_1S_2C_3 + \ell_3C_1C_2S_3\,.
\end{aligned}\right\} \tag{6.65}$$

The equation has two solutions φ_3 in terms of φ_2.

From the symmetry with respect to plane Σ it follows that φ_1 is uniquely determined by φ_2 and φ_3. An explicit expression for φ_1 in terms of φ_2 and φ_3 is obtained by evaluating the Woernle-Lee equation based on the product $\mathbf{n}_6 \cdot \mathbf{n}_4$. This is the equation $\mathbf{n}_k \cdot \mathbf{n}_{k-2} = \mathbf{n}_k \cdot \mathbf{n}_{k+4}$ with $k = 6$. Table 5.2 in combination with (6.60) yields the equation

$$s_1[S_3(c_2s_3 + C_2s_2c_3) + C_3S_2s_2]$$
$$= (1 - c_1)\Big[C_1S_3(s_2s_3 - C_2c_2c_3) + S_2(S_1S_3c_3 - C_1C_3c_2) - S_1C_2C_3\Big] \,, \quad (6.66)$$

whence it follows that

$$\tan\frac{\varphi_1}{2} = \frac{1 - c_1}{s_1} = \frac{S_3(c_2s_3 + C_2s_2c_3) + C_3S_2s_2}{C_1S_3(s_2s_3 - C_2c_2c_3) + S_2(S_1S_3c_3 - C_1C_3c_2) - S_1C_2C_3} \,. \quad (6.67)$$

An equation for $\tan\varphi_4/2$ is obtained in the same way by expressing the product $\mathbf{n}_3 \cdot \mathbf{n}_1$ in the two forms $\mathbf{n}_k \cdot \mathbf{n}_{k-2} = \mathbf{n}_k \cdot \mathbf{n}_{k+4}$ with $k = 3$. In view of the symmetry of Fig. 6.5 the equation is directly obtained by interchanging in (6.67) α_1 with α_3 and φ_2 with φ_3:

$$\tan\frac{\varphi_4}{2} = \frac{S_1(c_3s_2 + C_2s_3c_2) + C_1S_2s_3}{C_3S_1(s_2s_3 - C_2c_2c_3) + S_2(S_1S_3c_2 - C_1C_3c_3) - S_3C_2C_1} \,. \quad (6.68)$$

Example: The triple plane-symmetric mechanism shown in Fig. 4.6 is characterized by the parameters $\ell_1 = \ell_2 = \ell_3 = 1$, $h_2 = h_3 = 0$ and $\alpha_1 = \alpha_2 = \alpha_3 = \pi/2$. This is the special case with a single solution (φ_1, φ_3) for a given angle φ_2. Equations (6.64) and (6.67) are

$$c_2 + c_2c_3 + c_3 = 0 \,, \qquad \tan\frac{\varphi_1}{2} = \frac{c_2s_3}{c_3} \,. \quad (6.69)$$

With c_2 from the first equation the second becomes $\tan\varphi_1/2 = -s_3/(1+c_3)$ or $\varphi_1 = -\varphi_3$. Except for slightly different definitions of angles, the same results were obtained in (4.20) and (4.22). End of example.

6.4.3 Trihedral Bricard Mechanism

This mechanism was developed by Bricard [10] in search for a system having the property that in every position the six axes are lines of a special linear complex. Consider Fig. 6.6. The arbitrary spatial trihedral with lines 2, 4, 6 and with vertex A, referred to as trihedral A, is given. Furthermore, a point B is given. The perpendiculars 1, 3, 5 from B onto the three planes of trihedral A define the trihedral B. The construction implies that the lines 2, 4, 6 of trihedral A are perpendiculars of the three planes of trihedral B. With the labeling shown in Fig. 6.6 the line i ($i = 1, \ldots, 6$ cyclic) is normal to the plane of lines $i - 1$ and $i + 1$. Let P_2, P_4, P_6 and P_1, P_3, P_5 be the feet of the correspondingly labeled perpendiculars. They form the spatial polygon shown in dashed lines. The length of the side $\overline{\mathrm{P}_i\mathrm{P}_{i+1}}$ is called ℓ_i. The line segment $\overline{\mathrm{AP}_i}$ ($i = 1, 3, 5$) which is not shown is hypotenuse in the rectangular triangle (A,P_i,P_{i-1}) as well as in the rectangular triangle

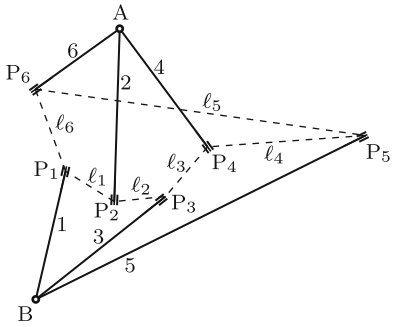

Fig. 6.6 Trihedrals A and B. Line i is normal to the plane of lines $i-1$ and $i+1$ ($i = 1, \ldots, 6$ cyclic)

(A,P_i,P_{i+1}). Consequently, $\overline{AP}_{i-1}^2 + \ell_{i-1}^2 = \overline{AP}_{i+1}^2 + \ell_i^2$ $(i = 1, 3, 5)$. This establishes the three equations

$$\ell_1^2 - \ell_6^2 = \overline{AP_6}^2 - \overline{AP_2}^2 , \quad \ell_3^2 - \ell_2^2 = \overline{AP_2}^2 - \overline{AP_4}^2 , \quad \ell_5^2 - \ell_4^2 = \overline{AP_4}^2 - \overline{AP_6}^2 . \tag{6.70}$$

Summation yields

$$\ell_1^2 + \ell_3^2 + \ell_5^2 = \ell_2^2 + \ell_4^2 + \ell_6^2 . \tag{6.71}$$

Imagine now the lengths $\ell_1, \ldots, \ell_6$ to be rigid rods interconnected by revolute joints at the points P_i $(i = 1, \ldots, 6)$. Each joint axis has the direction of the corresponding perpendicular i. This means that each rod carries two mutually perpendicular joint axes which are also perpendicular to the rod. The axes 2, 4, 6 intersect at the single point A, and the axes 1, 3, 5 intersect at the single point B. Proposition: Every mechanism composed of six rods and of six revolute joints having these orthogonality properties and arbitrary lengths $\ell_1, \ldots, \ell_6$ satisfying (6.71) has a single degree of freedom if one body is held fixed. This is the trihedral Bricard mechanism (sometimes also referred to as orthogonal Bricard mechanism). As is the case in the Bennett mechanism each joint has zero offset. Bricard's proof of mobility one is as follows. The construction of the system requires the specification of twelve parameters, namely, three coordinates for each of the points A and B and two direction cosines for each line of trihedral A. Six out of these twelve parameters determine the dimensions of the system and the remaining six its position in space. Of interest are only the first six parameters. Their number exceeds the number of independent lengths by one. The single free parameter constitutes the single degree of freedom. End of proof. Since in every position of the mechanism the six joint axes intersect the line $\overline{AB}$, they are lines of the special linear complex with the axis $\overline{AB}$. In Fig. 4.6 the special mechanism is shown in which the six lengths $\ell_1, \ldots, \ell_6$ are identical.

A trihedral Bricard mechanism can assume so-called planar positions, i.e., positions in which the polygon of points $P_1, \ldots, P_6$ is planar. In these positions three joint axes are normal to the plane. They intersect at infinity. The other three joint axes are lying in the plane. They either intersect at a single point or are parallel. The two rods coupled by any of these three joints are collinear. From this it follows that every planar position of the mechanism creates a triangle of rods in the plane. In order to find all planar positions with collinear pairs of rods, say pairs (1,2), (3,4) and (5,6), the altogether eight combinations of sums and differences $|\ell_1 \pm \ell_2|$, $|\ell_3 \pm \ell_4|$ and $|\ell_5 \pm \ell_6|$ are calculated. Each combination is checked whether it satisfies the triangle-inequalities. In the same way all planar positions with collinear pairs of rods (2,3), (4,5) and (6,1) are determined. With at least four of the altogether sixteen combinations of sums and differences the triangle-inequalities are satisfied. The proof is left to the reader. It makes use of (6.71).

Example: The mechanism with lengths $(\ell_1, \ell_2, \ell_3, \ell_4, \ell_5, \ell_6) = (16, 3, 9, 17, 5, 8)$ has the eight planar positions shown in Figs. 6.7a-h. In Fig. 6.7d all six rods are collinear, and the intersection points of both triples of joint axes are at infinity. End of example.

The figures reveal the existence of two different types of trihedral mechanisms. In Figs. 6.7a-d the number of differences of lengths in the triangle is odd, and in Figs. 6.7e-h the number of sums of lengths is odd. According to the rules in Fig. 5.1 the following quantities are defined:
– unit vectors $\mathbf{n}_1, \ldots, \mathbf{n}_6$ along the joint axes (sense of direction arbitrary)
– vectors $\ell_i \mathbf{a}_i = \overrightarrow{P_i P_{i+1}}$ $(i = 1, \ldots, 6)$
– constant angles α_i and joint variables φ_i $(i = 1, \ldots, 6)$.
The angles $\alpha_1, \ldots, \alpha_6$ are either $+\pi/2$ or $-\pi/2$. Simple inspection reveals that, no matter how $\mathbf{n}_1, \ldots, \mathbf{n}_6$ are directed, the number of positive angles $\alpha_i = +\pi/2$ is even in Figs. 6.7a-d and odd in Figs. 6.7e-h. Wohlhart [33] who presented the first complete kinematics analysis speaks of a type 2 mechanism in the former case and of a type 1 mechanism in the latter. A type 2 mechanism is obtained from type 1 and vice versa by opening one joint and by closing it again after giving one of the neighboring bodies a 180°-rotation about a normal to the joint axis.

Let $\mathbf{n}_1, \ldots, \mathbf{n}_6$ be directed such that $\alpha_i = +\pi/2$ $(i = 1, \ldots, 6)$ in type 2, and that $\alpha_1 = \alpha_3 = \alpha_5 = +\pi/2$, $\alpha_2 = \alpha_4 = \alpha_6 = -\pi/2$ in type 1. With the usual notation $C_i = \cos\alpha_i$, $S_i = \sin\alpha_i$ this means that $C_i = 0$ $(i = 1, \ldots, 6)$ and

$$\left.\begin{array}{ll} S_i = +1 \quad (i = 1, \ldots, 6) & (\text{type } 2)\,, \\ S_1 = S_3 = S_5 = +1\,, \quad S_2 = S_4 = S_6 = -1 & (\text{type } 1)\,. \end{array}\right\} \tag{6.72}$$

The characteristic parameter specifying the type is

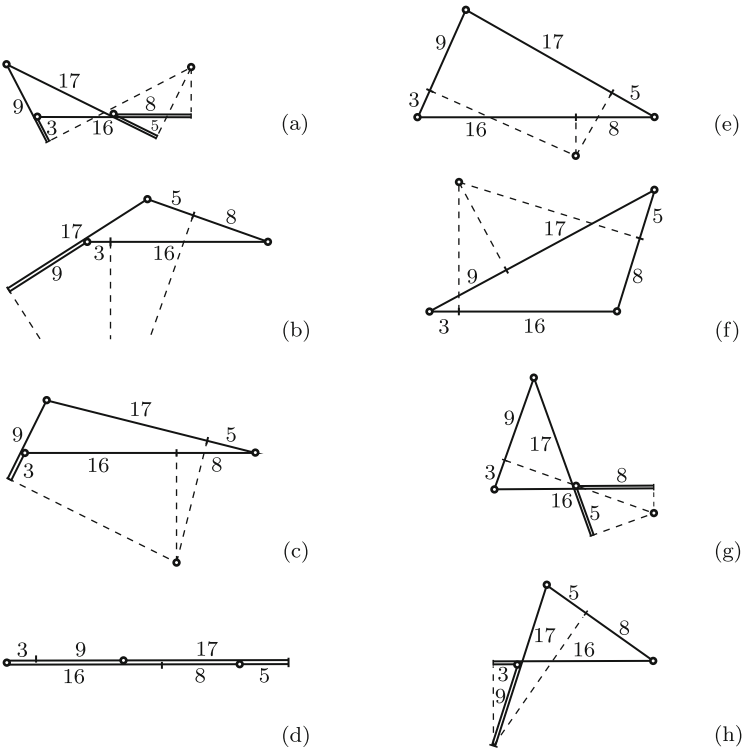

Fig. 6.7 The eight planar positions of the trihedral Bricard mechanism with lengths $(\ell_1, \ell_2, \ell_3, \ell_4, \ell_5, \ell_6) = (16, 3, 9, 17, 5, 8)$. Type 2 with odd number of differences of lengths **(Figs. a–d)** and type 1 with odd number of sums of lengths **(Figs. e–h)**

$$\lambda = S_i S_{i+1} \quad (\, i = 1, \ldots, 6 \text{ cyclic}\,) = \begin{cases} +1 & (\text{type } 2)\,, \\ -1 & (\text{type } 1)\,. \end{cases} \tag{6.73}$$

The following kinematics analysis is different from Wohlhart's. Three Woernle-Lee equations are formulated. Two equations are based on the products $\mathbf{n}_6 \cdot \mathbf{n}_4$ and $\mathbf{n}_6 \cdot \mathbf{n}_3$. They are written in the forms

$$\mathbf{n}_k \cdot \mathbf{n}_{k-2} = \mathbf{n}_k \cdot \mathbf{n}_{k+4} \qquad (k = 6)\,, \tag{6.74}$$

$$\mathbf{n}_k \cdot \mathbf{n}_{k-3} = \mathbf{n}_k \cdot \mathbf{n}_{k+3} \qquad (k = 6)\,. \tag{6.75}$$

The third equation is based on the product $\mathbf{r} \cdot \mathbf{n}_6 \times \mathbf{n}_4$ with $\mathbf{r}$ being the vector pointing from P_6 to P_4 . Since $\mathbf{r}$, $\mathbf{n}_6$ and $\mathbf{n}_4$ are coplanar, the Woernle-Lee equation splits into two equations:

$$\left.\begin{aligned} (\ell_6 \mathbf{a}_k + \ell_1 \mathbf{a}_{k+1} + \ell_2 \mathbf{a}_{k+2} + \ell_3 \mathbf{a}_{k+3}) \cdot \mathbf{n}_k \times \mathbf{n}_{k+4} &= 0\,, \\ (\ell_4 \mathbf{a}_{k-2} + \ell_5 \mathbf{a}_{k-1}) \cdot \mathbf{n}_k \times \mathbf{n}_{k-2} &= 0\,. \end{aligned}\right\} \quad (k = 6) \tag{6.76}$$

All equations are valid with indices changed cyclicly. Evaluation of (6.74) and (6.75) by means of Table 5.2 results in the equations

$$c_2 = -\frac{\lambda c_1 c_3 + c_5}{s_1 s_3} , \qquad s_2 = \frac{s_4 s_5}{s_1} = \frac{s_5 s_6}{s_3} . \tag{6.77}$$

The second expression for s_2 is the result of increasing all indices by one.

In the second Eq.(6.76) the vectors $(\ell_4 \mathbf{a}_{k-2} + \ell_5 \mathbf{a}_{k-1})$ and $\mathbf{n}_k \times \mathbf{n}_{k-2}$ have the coordinate matrices

$$\begin{bmatrix} \text{1st coordinate is irrelevant} \\ (\ell_4 c_5 + \ell_5) c_6 \\ -(\ell_4 c_5 + \ell_5) s_6 \end{bmatrix} , \quad \begin{bmatrix} 0 \\ S_4 s_5 s_6 \\ S_4 s_5 c_6 \end{bmatrix} , \tag{6.78}$$

respectively. Hence the second Eq.(6.76) is the identity. Not so the first equation. The vectors $(\ell_6 \mathbf{a}_k + \ell_1 \mathbf{a}_{k+1} + \ldots)$ and $\mathbf{n}_k \times \mathbf{n}_{k+4}$ have the coordinate matrices

$$\begin{bmatrix} \text{1st coordinate is irrelevant} \\ \ell_6 + \ell_1 c_1 + \ell_2 c_2 c_1 + \ell_3 (\lambda s_3 s_1 + c_3 c_2 c_1) \\ -S_1 S_6 s_2 (\ell_2 + \ell_3 c_3) \end{bmatrix} , \quad \begin{bmatrix} 0 \\ S_1 S_3 S_6 s_2 s_3 \\ S_3 (-\lambda c_3 s_1 + s_3 c_2 c_1) \end{bmatrix} , \tag{6.79}$$

respectively. The scalar product allows factoring out $S_1 S_3 S_6 s_2$. The first Eq.(6.76) then is the first of the six equations below. The remaining equations are obtained by cyclic permutation of indices.

$$\left.\begin{array}{ll} 1. & (\ell_2 c_3 + \ell_3) s_1 + \lambda (\ell_1 c_1 + \ell_6) s_3 = 0 , \\ 2. & (\ell_3 c_4 + \ell_4) s_2 + \lambda (\ell_2 c_2 + \ell_1) s_4 = 0 , \\ 3. & (\ell_4 c_5 + \ell_5) s_3 + \lambda (\ell_3 c_3 + \ell_2) s_5 = 0 , \\ 4. & (\ell_5 c_6 + \ell_6) s_4 + \lambda (\ell_4 c_4 + \ell_3) s_6 = 0 , \\ 5. & (\ell_6 c_1 + \ell_1) s_5 + \lambda (\ell_5 c_5 + \ell_4) s_1 = 0 , \\ 6. & (\ell_1 c_2 + \ell_2) s_6 + \lambda (\ell_6 c_6 + \ell_5) s_2 = 0 . \end{array}\right\} \tag{6.80}$$

Each equation involves two variables. The first equation yields φ_3 in terms of φ_1, and the fifth equation yields φ_5 in terms of φ_1. These equations have the forms

$$A_j \cos\varphi_j + B_j \sin\varphi_j = R_j \qquad (j = 3, 5) \tag{6.81}$$

with coefficients which are functions of φ_1. Each equation has two solutions φ_{3_k} and φ_{5_k} $(k = 1, 2)$. Their cosines and sines are

$$\left.\begin{array}{l} c_{j_k} = \dfrac{A_j R_j + (-1)^k B_j \sqrt{A_j^2 + B_j^2 - R_j^2}}{A_j^2 + B_j^2} , \\ s_{j_k} = \dfrac{B_j R_j - (-1)^k A_j \sqrt{A_j^2 + B_j^2 - R_j^2}}{A_j^2 + B_j^2} \end{array}\right\} \quad (j = 3, 5 \; ; \; k = 1, 2) . \tag{6.82}$$

By substituting coefficients it is verified that the square roots are identical: $A_3^2 + B_3^2 - R_3^2 - (A_5^2 + B_5^2 - R_5^2) = 0$ because of (6.71). Furthermore, by substituting the expressions (6.82) it is verified that the third Eq.(6.80) is satisfied by the combinations $(\varphi_{3_1}, \varphi_{5_1})$ and $(\varphi_{3_2}, \varphi_{5_2})$.

The first Eq.(6.77) determines for each of the two solutions c_3, s_3, c_5 the corresponding cosine c_2 and hence two angles $\pm\varphi_2$. The corresponding cosine c_4 is obtained by substituting the first expression $s_2 = s_4 s_5 / s_1$ into the second Eq.(6.80) and by deleting the common factor s_4. In the same way the corresponding cosine c_6 is obtained from the second expression for s_2 in combination with the sixth Eq.(6.80). The results are

$$c_4 = -\frac{\lambda s_1(\ell_2 c_2 + \ell_1) + \ell_4 s_5}{\ell_3 s_5}, \qquad c_6 = -\frac{\lambda s_3(\ell_1 c_2 + \ell_2) + \ell_5 s_5}{\ell_6 s_5}. \tag{6.83}$$

The signs of s_4 and s_6 are determined from (6.77). If s_2 changes sign, also s_4 and s_6 change signs. These results are summarized as follows. For every value of φ_1 there exist four (not necessarily real) sets of solutions $(\sigma\varphi_{2_i}, \varphi_{3_i}, \sigma\varphi_{4_i}, \varphi_{5_i}, \sigma\varphi_{6_i})$ $(i = 1, 2; \sigma = \pm 1)$. Equations (6.77) and (6.83) fail in planar positions characterized by either $s_1 = s_3 = s_5 = 0$ or by $s_2 = s_4 = s_6 = 0$. In these cases, the joint angles are determined from triangles (see Fig. 6.7).

Example: For the lengths $(\ell_1, \ell_2, \ell_3, \ell_4, \ell_5, \ell_6) = (16, 3, 9, 17, 5, 8)$ and for $\varphi_1 = 80°$ a type 1 mechanism has the solutions
$(\varphi_2, \varphi_3, \varphi_4, \varphi_5, \varphi_6) \approx (\sigma 36.8°, 142.9°, \sigma 48.4°, 127.9°, \sigma 27.3°)$ and
$(\sigma 92.8°, 67.8°, \sigma 98.3°, 83.7°, \sigma 111.5°)$ $(\sigma = \pm 1)$. End of example.

Example: The trihedral mechanism in Fig. 4.6 is a type 1 mechanism with identical lengths $\ell_i \equiv 1$ $(i = 1, \ldots, 6)$. It has four planar positions. Equations (6.80) reduce to

$$\left.\begin{array}{ll} 1. & (c_3+1)s_1 - (c_1+1)s_3 = 0, \\ 2. & (c_4+1)s_2 - (c_2+1)s_4 = 0, \\ 3. & (c_5+1)s_3 - (c_3+1)s_5 = 0, \\ 4. & (c_6+1)s_4 - (c_4+1)s_6 = 0, \\ 5. & (c_1+1)s_5 - (c_5+1)s_1 = 0, \\ 6. & (c_2+1)s_6 - (c_6+1)s_2 = 0. \end{array}\right\} \tag{6.84}$$

For a given angle φ_1 these equations and (6.77) have a single solution only, namely, $\varphi_3 = \varphi_5 = \varphi_1$, $\varphi_4 = \varphi_6 = \varphi_2$ and $c_1 + c_1 c_2 + c_2 = 0$. Except for slightly different definitions of angles, the same results were obtained in (4.20) and (4.22). Compare also the first Eq.(6.84) with (4.23). End of example.

With six rods of mutually different lengths altogether six different sequences and with each sequence both types of mechanism can be formed. In general, the numbers of planar positions are different for different sequences and for different types. Example: The sequence of lengths in Figs. 6.7a-h is

the first of the following six sequences which represent all possible mechanisms which can be formed with these lengths:

$$\left.\begin{matrix}(16,3,9,17,5,8)\\(16,8,9,17,5,3)\end{matrix}\right\}\ \text{(a)}\ ,\quad \left.\begin{matrix}(16,17,9,8,5,3)\\(16,17,9,3,5,8)\end{matrix}\right\}\ \text{(b)}\ ,\quad \left.\begin{matrix}(16,8,9,3,5,17)\\(16,3,9,8,5,17)\end{matrix}\right\}\ \text{(c)}\ .$$

It is left to the reader to verify the following statements. With each of the sequences (a) both types have four planar positions. With each of the sequences (b) both types have two planar positions. With each of the sequences (c) there are two planar positions of type 1 and three of type 2.

Condition (6.71) is $A+B+C=0$ with $A=(\ell_1-\ell_2)(\ell_1+\ell_2)$, $B=(\ell_3-\ell_4)(\ell_3+\ell_4)$, $C=(\ell_5-\ell_6)(\ell_5+\ell_6)$. Nonzero integer solutions $(\ell_1,\ell_2,\ell_3,\ell_4,\ell_5,\ell_6)$ are obtained from numbers A, B, $C=-(A+B)$ which are products of two different even or two different odd numbers. Example: $A=2\cdot 8$, $B=1\cdot 17$, $C=-1\cdot 33=-3\cdot 11$ yield $(\ell_1,\ell_2,\ell_3,\ell_4,\ell_5,\ell_6)=(5,3,9,8,16,17)$ and $(5,3,9,8,4,7)$.

Condition (6.71) is satisfied by the lengths $\ell_1=a$, $\ell_2=a+b$, $\ell_3=a+2b+c$, $\ell_4=a+c$, $\ell_5=a+b+2c$, $\ell_6=a+2b+2c$ (a,b,c arbitrary). Example: $a=b=1$, $c=2$ yield $(\ell_1,\ell_2,\ell_3,\ell_4,\ell_5,\ell_6)=(1,2,5,3,6,7)$. The mechanism with these lengths has seven planar positions (four of type 2). In one planar position of type 1 and in one of type 2 all six lengths are collinear.

6.4.4 Dietmaier's Mechanism

The ideas and results presented in this section are due to Dietmaier [19]. The analysis of the 7R mechanism in Sect. 5.4.7 resulted in a 16th-order equation for the variable $x_1=\tan\varphi_1/2$ with coefficients depending on the variable φ_7 and on constant Denavit-Hartenberg parameters. A prescribed value of φ_7 (arbitrary) determines up to sixteen real roots x_1. The 16th-order equation describes a 6R mechanism when the parameters and variables of body 7 and of joint 7 are set equal to zero: $\ell_7=h_7=0$, $\alpha_7=0$, $\varphi_7\equiv 0$ (see Fig. 5.7). This has the consequence that the coefficients of the 16th-order equation are constants. Since x_1 is variable, all seventeen coefficients must be zero. This requirement establishes seventeen conditions on the Denavit-Hartenberg parameters ℓ_i, h_i, α_i ($i=1,\ldots,6$; $\ell_1=1$ without loss of generality). The 16th-order equation remains valid when the indices of all parameters and all variables are cyclicly increased by $k=1,2,3,4,5$. Hence altogether $6\times 17=102$ conditions must be satisfied. Dietmaier's numerical search for Denavit-Hartenberg parameters satisfying these conditions led to a new family of overconstrained 6R mechanisms. The parameters must satisfy the following complicated symmetry relationships.

1. The opposite bodies 1 and 4 are identical:

$$\ell_4 = \ell_1 \,, \qquad \alpha_4 = \alpha_1 \,. \tag{6.85}$$

2. The opposite joints 2 and 5 have zero offset:

$$h_2 = 0 \,, \qquad h_5 = 0 \,. \tag{6.86}$$

3. Joints 1 and 3 and joints 4 and 6 have pairwise identical offsets:

$$h_3 = h_1 \,, \qquad h_6 = h_4 \,. \tag{6.87}$$

4. Bodies 2 and 3 and the opposite bodies 5 and 6 have pairwise identical ratios

$$\frac{\ell_2}{\sin\alpha_2} = \frac{\ell_3}{\sin\alpha_3} \,, \qquad \frac{\ell_5}{\sin\alpha_5} = \frac{\ell_6}{\sin\alpha_6} \,. \tag{6.88}$$

5. These ratios are subject to the symmetrical constraint equation

$$\frac{\ell_2}{\sin\alpha_2}(\cos\alpha_2 + \cos\alpha_3) = \frac{\ell_5}{\sin\alpha_5}(\cos\alpha_5 + \cos\alpha_6) \,. \tag{6.89}$$

The last three equations can be used for expressing ℓ_3, ℓ_5 and ℓ_6 in terms of ℓ_2, α_2, α_3, α_5 and α_6. With the usual notation $C_i = \cos\alpha_i$ and $S_i = \sin\alpha_i$

$$\ell_3 = \ell_2 \frac{S_3}{S_2} \,, \qquad \ell_5 = \ell_2 \frac{S_5(C_2 + C_3)}{S_2(C_5 + C_6)} \,, \qquad \ell_6 = \ell_2 \frac{S_6(C_2 + C_3)}{S_2(C_5 + C_6)} \,. \tag{6.90}$$

Let φ_1 be the independent variable. The associated solutions for φ_2, φ_4, φ_5, φ_6 are determined from (5.94) and (5.93) after setting $\ell_7 = h_7 = 0$, $\alpha_7 = 0$, $\varphi_7 \equiv 0$. The matrices $\underline{A}$, $\underline{B}$ and $\underline{P}$ are constants. The matrix $\underline{u}_r$ is defined in (5.80). One out of the four Eqs.(5.94) is solved for x_6. Substitution into the other equations results in three equations which are quadratic in the sines and cosines of φ_1 and φ_2. Hence they have the forms

$$A_i \sin^2\varphi_2 + B_i \sin\varphi_2 \cos\varphi_2 + C_i \sin\varphi_2 + D_i \cos^2\varphi_2 + E_i \cos\varphi_2 + F_i = 0 \tag{6.91}$$

$(i = 1, 2, 3)$ with coefficients which are functions of φ_1. The equations are fourth-order equations for the variable $x_2 = \tan\varphi_2/2$ (see (5.60)). Only those solutions x_2 which are common to all three equations determine relevant angles φ_2. Once φ_2 is known also $\varphi_6 = 2\tan^{-1} x_6$ is known and then also φ_4 and φ_5 from $\underline{y}$ (see (5.93)). Dietmaier's numerical investigations revealed that his 6R mechanism has up to four different configurations for a given value of the independent variable no matter which angle is chosen as independent variable. In this respect the mechanism is different from all other known 6R mechanisms.

6.5 Mobile Polyhedra

Euler expressed, without mathematical arguments, the conviction that all polyhedra are rigid. By this the following is meant. In a polyhedron every face is interpreted as rigid body and every edge as revolute joint. Nonrigid means that the polyhedron is a mobile mechanism. Cauchy proved that all convex polyhedra are, indeed, rigid (see Demaine/O'Rourke [17]). Bricard [10] constructed mobile nonconvex octahedra which are self-intersecting. Connelly constructed the first nonconvex polyhedron capable of moving without self-intersection. Stimulated by this achievement Steffen constructed simpler ones (see Connelly [14]). The simplest one is constructed as follows (see Fig. 6.8). Starting point is the rigid isosceles triangle $(A_1, 0, A_2)$ in the plane E with leg lengths ℓ and with vertex angle α. On the perpendicular to E through 0 the point B_1 is marked at an arbitrary distance h from 0. Rods of equal length a connect A_1 and A_2 with B_1. Two more rods of equal length b connect A_1 and A_2 with a point B_2 on the dashed bisector of the angle α. In the next step, congruent triangles (A_1,B_1,C_1) and (A_1,B_2,C_1) are constructed as follows. To B_1 a rod of length b is attached and to B_2 a rod of length a. The point C_1 connecting these rods is located on a circle in a plane normal to the line $\overline{B_1B_2}$ and with its center on this line. With a given length $\overline{A_1C_1} = c$ (arbitrary) there are two possible locations for C_1. One of them is chosen arbitrarily. Let C_1^* be the other point not chosen. Repetition of this construction produces two more triangles (A_2,B_1,C_2) and (A_2,B_2,C_2) which are congruent to the previous ones. Of the two possible locations for C_2 the one is chosen with which the dashed line $\overline{C_1C_2}$ is not parallel to $\overline{A_1A_2}$. Let C_2^* be the other point not chosen.

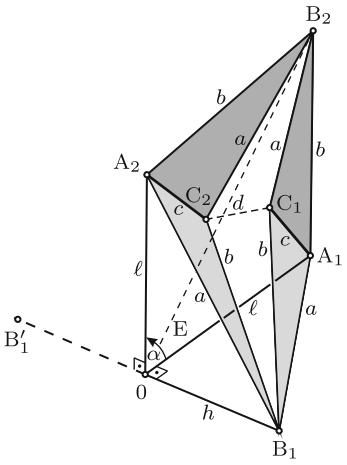

Fig. 6.8 One half of a mobile polyhedron

Now, imagine the connections of rods at the points A_1, A_2, B_1 and B_2 to be spherical joints. The system thus defined has the degree of freedom one. The rigid isosceles triangle (A_1,A_2,B_2) can rotate (in a limited angular range) about its base line $\overline{A_1A_2}$. This rotation forces C_1 and C_2 to move along certain trajectories. During this motion the distance of these two points is not constant. Now, C_1 and C_2 are connected by a rod of fixed length d. In order to restore the degree of freedom the angle α is made variable by connecting the rods $\overline{0A_1}$ and $\overline{0A_2}$ at 0 by a spherical joint.

The 1-d.o.f. system thus constructed consists of the rigid triangles $(0,A_1,B_1)$, $(0,A_2,B_1)$, (A_1,B_1,C_1), (A_1,B_2,C_1), (A_2,B_1,C_2), (A_2,B_2,C_2), (B_1,C_1,C_2) and (B_2,C_1,C_2). This system is one half of the desired polyhedron. The other half is obtained in two steps. First step: The existing halfpolyhedron - placed in the position with B_2 in E - is reflected in E. Second step: The reflections of C_1 and C_2 are replaced by the reflections of C_1^* and of C_2^*, respectively. With the reflection B_1' of B_1 the triangular faces (B_1,B_1',A_1) and (B_1,B_1',A_2) of the polyhedron are produced.

With suitably chosen lengths h, a, b, c, d B_2 is able to move along a short segment of a trajectory on either side of E without causing a collision of faces of the polyhedron. In [14] the lengths are proposed: $2h = 17$, $a = 12$, $b = 10$, $c = 5$, $d = 11$. The polyhedron can be produced by folding the symmetric figure shown in Fig. 6.9. The polyhedron has $n = 14$ faces (bodies) and $m = 21$ edges (revolute joints). With these numbers Grübler's formula (4.1) yields the degree of freedom $F = -27 + d$. Since F equals one, the system of altogether 5×21 constraint equations has the defect $d = 28$. See http://www.mathematik.com/Steffen/ for a display of the motion.

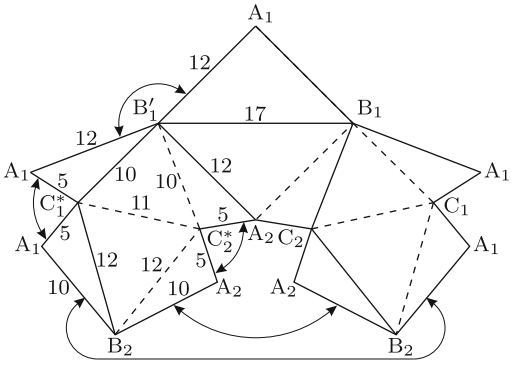

Fig. 6.9 Cutting and folding instructions for Steffen's mobile polyhedron. Valley folds in dashed lines. Mountain folds in solid lines

6.6 RRCRP Mechanism

A closed kinematic chain RRCRP has six joint variables. Hence it is rigid unless it is overconstrained. It will be seen that the special chain shown in Fig. 6.10 is overconstrained with degree of freedom one. The assembly position shown is characterized as follows. The axis of the revolute R_4 is orthogonal to the x, y-plane of the frame-fixed x, y, z-system with origin 0. The other four joint axes are in this plane (the prismatic joint P parallel to the revolute R_1 at $y = \ell = \text{const}$; the axes of the revolutes R_1 and R_2 and of the cylindrical joint C intersecting at 0; R_1 and R_2 under an angle $\alpha = \text{const}$ and R_2 and C orthogonally). After a rotation through φ_1 (arbitrary) in R_1 the unit vector $\mathbf{n}_2$ along the axis of R_2 has the coordinates $\underline{n}_2 = [\cos\alpha \quad -\sin\alpha\sin\varphi_1 \quad -\sin\alpha\cos\varphi_1]$. Dependent on φ_1 the angle φ_2 in R_2 and the translatory variable in joint C can be determined such that the vector $\mathbf{r}$ pointing to the revolute R_4 has the required coordinates $y = \ell$ and $z = 0$. Moreover, the angle φ_3 in joint C can be determined such that the axis of R_4 has the required direction orthogonal to the x, y-plane. This proves that the mechanism has the degree of freedom one, and that φ_1 can be used as independent input variable. As output the translatory variable in the prismatic joint P is chosen. Let this be the coordinate x of $\mathbf{r}$. From the orthogonality condition $\mathbf{n}_2 \cdot \mathbf{r} = 0$ it follows that

$$x = \ell \tan\alpha \sin\varphi_1 \ . \tag{6.92}$$

Rotation with constant angular velocity $\dot{\varphi}_1 = \omega$ is converted into oscillatory translation $x(t) = \ell \tan\alpha \sin\omega t$. The mechanism was used in a pneumatic saw (see *Design and development/scanning the field for ideas*, Sept.1964, p.158). See also Altmann [2, 1].

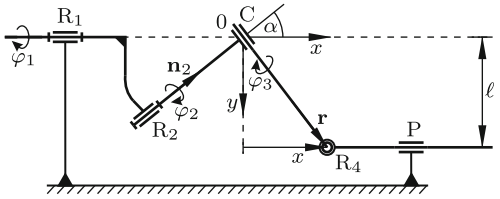

Fig. 6.10 Mechanism $R_1R_2CR_4P$ converting rotation into harmonic translation

6.7 4R-P Mechanism

In the fixed x, y, z-system of Fig. 6.11a two skew lines n_1 and n_2 are fixed. Their common perpendicular of length ℓ lies in the z-axis. This axis is intersected by n_1 at $z = \ell/2$ (point A_1) and by n_2 at $z = -\ell/2$ (point A_2). The projected angle α between the lines is bisected by the y-axis. The lines n_1 and n_2 are the axes of two cylinders 1 and 2 of equal radius r. Points denoted B_1 and B_2 are fixed on the cylinders. More precisely, B_i $(i = 1, 2)$ is fixed on cylinder i such that the line $\overline{\mathrm{A}_i\mathrm{B}_i}$ is orthogonal to both n_i and z-axis, and that, furthermore, B_1 and B_2 are, in the projection shown, on a line parallel to the y-axis and at equal distances from the x-axis. Imagine now that both cylinders are rotated about their axes through identical angles φ (arbitrary). This causes B_1 and B_2 to move on their respective circles to new positions B'_1, B'_2. The displacements in z-direction are identical, namely, $u = r \sin\varphi$, and also the displacements in x-direction are identical, namely, $r(1 - \cos\varphi)$. In the projection shown the distance between B'_1 and B'_2 is $\delta = 2r \cos\varphi \sin\alpha/2$. The generator of cylinder i passing through B'_i is called n'_i $(i = 1, 2)$. In Fig. 6.11b the essential points and lines are shown in the projection along the x-axis. In this projection, the axes and generators of the cylinders are shown as lines parallel to the y-axis. Through B'_1 and B'_2 lines $\overline{\mathrm{B}'_1\mathrm{C}_1}$ and $\overline{\mathrm{B}'_2\mathrm{C}_2}$ of equal lengths $\ell/2$ are drawn parallel to the z-axis. The line p through C_1 and C_2 is (not only in this projection) parallel to the y-axis.

Imagine now that $\overline{\mathrm{A}_1\mathrm{A}_2}$, $\overline{\mathrm{A}_1\mathrm{B}'_1}$, $\overline{\mathrm{A}_2\mathrm{B}'_2}$, $\overline{\mathrm{B}'_1\mathrm{C}_1}$ and $\overline{\mathrm{B}'_2\mathrm{C}_2}$ are rigid links which are interconnected by four revolute joints with pairwise parallel axes n_1, n'_1 and n_2, n'_2 and by a prismatic joint with the axis p. The result is a spatial overconstrained single-degree-of-freedom mechanism

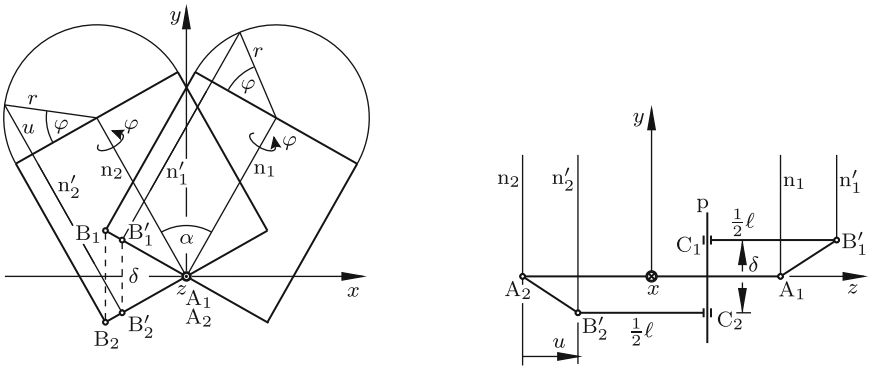

Fig. 6.11 4R-P mechanism projected along the z-axis **(a)** and along the x-axis **(b)**

4R-P with only five joint variables. The variable φ is identical in all four revolute joints. The joint variable in the prismatic joint is δ. It is independent of ℓ. This mechanism was described first by Mavroidis/Roth [27] (see also Mavroidis/Beddows [28]). The links need not have the shapes shown in the figures. Every link can be given any shape provided its two Denavit-Hartenberg parameters (length of the common perpendicular and projected angle of the two joint axes on the link) have the correct values. The link coupling the parallel axes n_1 and n_1', for example, can be placed anywhere between these axes. With this freedom of design it is possible to achieve full-cycle mobility in the revolute joints without collision of links and joint axes. The prismatic joint must be designed such that the passage through $\delta = 0$ is possible. In the special case $\alpha = 0$, the mechanism is the planar foldable four-bar in parallelogram configuration.

The mechanism is a simple means of converting the angular velocity $\dot{\varphi}$ about the fixed input axis n_1 into an identical angular velocity about the fixed skew output axis n_2 the location of which can be freely chosen by specifying the two design parameters α and ℓ. The mechanism is simpler and less expensive than a set of hypoid gears serving the same purpose. This is particularly true when ℓ is large. However, like the planar foldable four-bar the mechanism is not well suited for transmitting a large torque from the input to the output axis.

6.8 Bricard-Borel Mechanism

The system shown in Fig. 6.12a consists of two parallel circular discs 1 and 2 (radii R_1 and $r_1 \neq R_1$ arbitrary) and of $n \geq 5$ rods of equal length ℓ_1 connecting the discs. The rods are generators of a frustum of a regular cone. The system is shown in two projections. The endpoints P_i and Q_i of the rods $i = 1, \ldots, n$ are connected to the discs by spherical joints. Disc 1 is a fixed base. Disc 2 is referred to as platform. Every rod is free to rotate about its longitudinal axis. This degree of freedom is not of interest. Because of the symmetry of the arrangement it is obvious that the platform has a single degree of freedom. It is free to undergo a continuous screw motion about the vertical z-axis with an independent angular variable φ and with a translatory variable z which is a function $z(\varphi)$. This function is obtained from Fig. 6.12b which shows the vertical projection in a position φ (arbitrary). In the x, y, z-system the endpoints P_1 and Q_1 of rod 1 have the coordinates $[R_1 \;\; 0 \;\; 0]$ and $[r_1 \cos\varphi \;\; r_1 \sin\varphi \;\; z]$, respectively. The condition of constant rod length establishes between z and φ the constraint equation $(r_1 \cos\varphi - R_1)^2 + r_1^2 \sin^2\varphi + z^2 = \ell_1^2$. Hence

$$z(\varphi) = \sqrt{2R_1 r_1 \cos\varphi + \ell_1^2 - (R_1^2 + r_1^2)} \,. \tag{6.93}$$

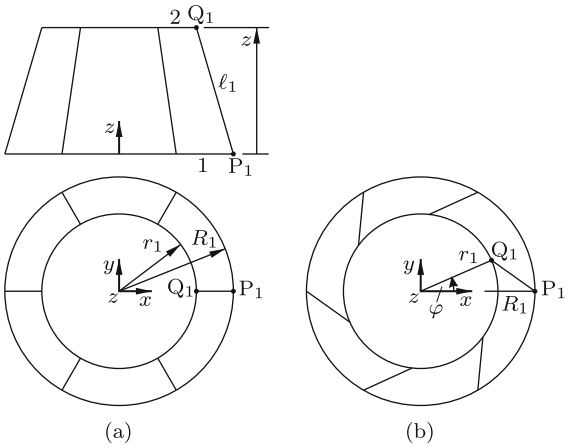

Fig. 6.12 Platform mounted on rods in positions $\varphi = 0$ **(a)** and $\varphi \neq 0$ **(b)**

The same function $z(\varphi)$ is obtained with arbitrary parameters R, r, ℓ satisfying the conditions

$$Rr = R_1 r_1 \,, \qquad \ell^2 = \ell_1^2 - (R_1^2 + r_1^2) + (R^2 + r^2) \,. \tag{6.94}$$

The same function $z(\varphi)$ is also obtained if both endpoints of a rod, i.e., the entire rod, are vertically lifted or lowered by an arbitrary amount (each rod by an individual amount). Also, because of the symmetry of the equations, it is immaterial whether the larger or the smaller radius is located on the platform. The degree of freedom one remains unchanged if an arbitrary number of rods each satisfying the said conditions is added to the system. Every point of the three-dimensional platform can be connected by a rod with a point of the base which is uniquely determined by the conditions. From this it follows that every point of the platform is moving on a base-fixed sphere. Platform-fixed points of the screw axis move on spheres with infinite radius. Conversely, every point fixed on the base moves on a platform-fixed sphere. All rods are lines of the linear complex with the given screw axis and with the pitch $p = \mathrm{d}z/\mathrm{d}\varphi$. These characteristics of the system were first discovered by Bricard [11] and Borel [9]. See also Husty/Zsombor-Murray [23].

6.9 Hyperboloid and Paraboloid Mechanisms

The hyperboloid of one sheet (Fig. 6.13a) and the hyperbolic paraboloid (Fig. 6.13b) have, in the cartesian x_1, x_2, x_3-systems shown, the equations

$$\text{hyperboloid of one sheet}: \qquad \frac{x_1^2}{a^2} + \frac{x_2^2}{b^2} - \frac{x_3^2}{c^2} = 1 \,, \tag{6.95}$$

$$\text{hyperbolic paraboloid}: \qquad \frac{x_1^2}{a^2} - \frac{x_2^2}{b^2} = x_3 \,. \tag{6.96}$$

Planes $x_1 = \text{const}$ and $x_2 = \text{const}$ intersect the hyperboloid in hyperbolas and the hyperbolic paraboloid in parabolas. Planes $x_3 = \text{const}$ intersect the hyperboloid in ellipses and the hyperbolic paraboloid in hyperbolas (in straight lines in the case $x_3 = 0$). Both surfaces are ruled surfaces, more specifically the only ruled surfaces having the property that every point is the intersection of two generating lines. The two families of generators of the hyperboloid, referred to as regulus 1 and regulus 2, have the equations (the parameters u and v are arbitrary constants; see Bronstein/Semendjajev/Musiol/Mühlig [12])

$$\left.\begin{array}{ll} \text{regulus 1}: & \dfrac{x_1}{a} + \dfrac{x_3}{c} = u\Big(1 + \dfrac{x_2}{b}\Big) \,, \quad u\Big(\dfrac{x_1}{a} - \dfrac{x_3}{c}\Big) = 1 - \dfrac{x_2}{b} \,, \\ \text{regulus 2}: & \dfrac{x_1}{a} + \dfrac{x_3}{c} = v\Big(1 - \dfrac{x_2}{b}\Big) \,, \quad v\Big(\dfrac{x_1}{a} - \dfrac{x_3}{c}\Big) = 1 + \dfrac{x_2}{b} \,. \end{array}\right\} \tag{6.97}$$

The corresponding equations for the paraboloid are

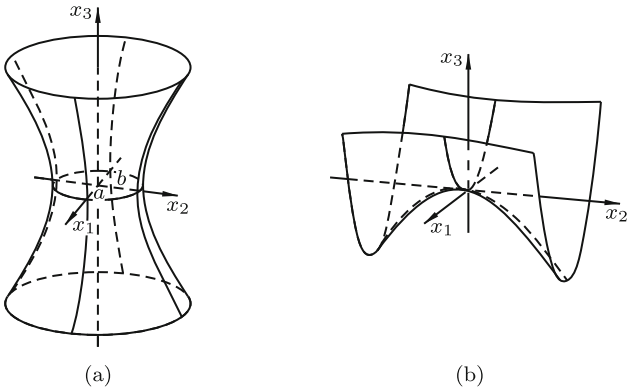

Fig. 6.13 Hyperboloid of one sheet **(a)** and hyperbolic paraboloid **(b)**

$$\left.\begin{array}{ll} \text{regulus 1}: & \dfrac{x_1}{a} + \dfrac{x_2}{b} = u \,, \quad u\Big(\dfrac{x_1}{a} - \dfrac{x_2}{b}\Big) = x_3 \,, \\ \text{regulus 2}: & \dfrac{x_1}{a} - \dfrac{x_2}{b} = v \,, \quad v\Big(\dfrac{x_1}{a} + \dfrac{x_2}{b}\Big) = x_3 \,. \end{array}\right\} \tag{6.98}$$

Hyperboloid of one Sheet

Equations (6.97) reveal the following properties of generators. Two generators belonging to one and the same regulus are skew. Every generator of

one regulus intersects all generators of the other regulus and exactly one of them at infinity. Three generators belonging to one and the same regulus are not parallel to one and the same plane. Three such generators determine a hyperboloid uniquely.

Imagine now that arbitrarily many (in the limit all) generators are rigid rods. Moreover, imagine that at every intersection point of any two such rods the respective rods are connected by a spherical joint (in the limit there is a spherical joint at every point of the hyperboloid). Proposition: The system of rods thus defined is an overconstrained mechanism having a single degree of freedom. It can move in such a way that in every position the rods are generators of a hyperboloid of one sheet. The intersections of all these hyperboloids with the plane $x_3 = 0$ are confocal ellipses.

Proof (see Bricard [10] and Hilbert/Cohn-Vossen [21]): It must be shown that the distance of any two spherical joints P and Q on an arbitrarily chosen rod is invariant under this motion. For this purpose (6.95) is written in the form

$$\sum_{i=1}^{3} \frac{x_i^2}{a_i - \lambda} = 1 \qquad (a_3 \le \lambda \le a_2 \le a_1 \quad \text{arbitr.}) \,. \tag{6.99}$$

Let p_i and q_i $(i = 1, 2, 3)$ be the coordinates of two points P and Q, respectively, on an arbitrary generator. Also the midpoint with coordinates $(p_i + q_i)/2$ $(i = 1, 2, 3)$ lies on this generator and, consequently on the surface. Hence

$$\sum_{i=1}^{3} \frac{p_i^2}{a_i - \lambda} = 1 \,, \qquad \sum_{i=1}^{3} \frac{q_i^2}{a_i - \lambda} = 1 \,, \qquad \sum_{i=1}^{3} \frac{(p_i + q_i)^2}{a_i - \lambda} = 4 \,. \tag{6.100}$$

From the third equation twice the sum of the first two equations is subtracted:

$$\sum_{i=1}^{3} \frac{(p_i - q_i)^2}{a_i - \lambda} = 0 \,. \tag{6.101}$$

Let r be the distance of the points P and Q. With (6.101)

$$r^2 = \sum_{i=1}^{3} (p_i - q_i)^2 = \sum_{i=1}^{3} (a_i - \lambda) \frac{(p_i - q_i)^2}{a_i - \lambda} = \sum_{i=1}^{3} a_i \frac{(p_i - q_i)^2}{a_i - \lambda} \,. \tag{6.102}$$

In (6.99) λ is replaced by an arbitrary λ' satisfying the conditions $a_3 \le \lambda' \le a_2$. The two hyperboloids with λ and with λ' are referred to as surface F and surface F$'$, respectively. The coordinates x_1', x_2', x_3' of points on F$'$ are generated from the coordinates x_1, x_2, x_3 of F by the affine transformation

$$x_i' = x_i \sqrt{\frac{a_i - \lambda'}{a_i - \lambda}} \qquad (i = 1, 2, 3) \,. \tag{6.103}$$

This transformation associates to the points P and Q of F points P′ and Q′, respectively, of F′ having the coordinates

$$p_i' = p_i\sqrt{\frac{a_i-\lambda'}{a_i-\lambda}}\,, \qquad q_i' = q_i\sqrt{\frac{a_i-\lambda'}{a_i-\lambda}} \qquad (i=1,2,3)\,. \tag{6.104}$$

For the distance r' of these points (6.102) is valid with the quantities bearing the prime. With (6.104)

$$r'^2 = \sum_{i=1}^{3} a_i\,\frac{(p_i'-q_i')^2}{a_i-\lambda'} = \sum_{i=1}^{3} a_i\,\frac{(p_i-q_i)^2}{a_i-\lambda} \equiv r^2\,. \tag{6.105}$$

This identity proves the invariance of the distance of points. The mechanism of rods which, in its initial position, is assembled on the hyperboloid F governed by (6.99) with given constants $a_3 \le \lambda \le a_2 \le a_1$ is able to assume a position in which it is located on a hyperboloid F′ governed by the same equation with the same constants $a_3 \le a_2 \le a_1$ and with an arbitrary $a_3 \le \lambda' \le a_2$.

The hyperboloid with the free parameter λ' intersects the plane $x_3 = 0$ in the ellipse depending on λ': $x_1^2/(a_1-\lambda') + x_2^2/(a_2-\lambda') = 1$. Its focal points are located on the x_1-axis symmetrically to the origin. Their distance is $\sqrt{(a_1-\lambda')-(a_2-\lambda')} = \sqrt{a_1-a_2}$ independent of λ'. Hence the ellipses are confocal. End of proof.

In the limit $\lambda' = a_2$ the ellipse degenerates to the line connecting the focal points. In this case, all rods lie in the x_1, x_3-plane and tangent to the hyperbola $x_1^2/(a_1-a_2) - x_3^2/(a_2-a_3) = 1$. In the limit $\lambda' = a_3$ all rods lie in the x_1, x_2-plane and tangent to the ellipse $x_1^2/(a_1-a_3) + x_2^2/(a_2-a_3) = 1$.

The hyperbolic paraboloid, too, is a 1-d.o.f. mechanism when all generators are interconnected by spherical joints at every point of intersection. By the same line of arguments it is proved that in every position the mechanism is a hyperbolic paraboloid with the equation depending on the free parameter λ:

$$\sum_{i=1}^{2} \frac{x_i^2}{a_i-\lambda} = x_3 \qquad (a_2\,,\ a_3 = \text{const}\,,\ \ a_2 \le \lambda \le a_3\,)\,. \tag{6.106}$$

Hyperbolic Mechanism for the Generation of a Plane

The minimal system of rods constituting a hyperbolic mechanism consists of five rods (see Fig. 6.14). Two skew rods g and g_1 representing generators of regulus 1 are interconnected by three rods of constant lengths (generators of regulus 2). The spherical joints on g and g_1 may be placed arbitrarily subject only to the inequality condition $\overline{P_1P_2} : \overline{P_1P_3} \neq \overline{Q_1Q_2} : \overline{Q_1Q_3}$ (in the case of equality the five lines would be generators of a hyperbolic paraboloid). Every generator of regulus 2 intersects all generators of regulus 1 and exactly one of them at infinity. Hence there exist a single generator of regulus 2 parallel

to g and a uniquely defined intersection point of this generator with g_1. Let Q be this point. When the 1-d.o.f.-mechanism is moving, each joint Q_i is moving on a sphere around P_i $(i = 1, 2, 3)$. Point Q, in particular, is moving on a sphere of infinite radius, i.e., in a plane E normal to g. Let 0 be the point where g intersects E. When E and g are held fixed as is shown in Fig. 6.14, the mechanism has the additional degree of freedom of rotation about g. Hence Q is free to move (in a certain ring-shaped region) in the fixed plane E. This generation of a plane by a mechanism having only spherical joints represents a spatial analog to the generation of a straight line by a Peaucellier inversor (see Sect. 17.13).

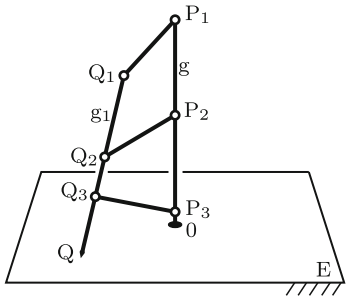

Fig. 6.14 Hyperbolic mechanism for the generation of a plane

6.10 Cam Mechanism

De la Hire is the author of

Theorem 6.2. *Mutually orthogonal tangents to an ellipse with semi axes a and b (arbitrary) intersect on the circle of radius* $\sqrt{a^2 + b^2}$ *about the center of the ellipse.*

Proof (see Fig. 6.15): In the x, y-system of principal axes the ellipse has the equation

$$\frac{x^2}{a^2} + \frac{y^2}{b^2} = 1 \tag{6.107}$$

and also the parameter equation

$$x = a\cos\psi\,, \qquad y = b\sin\psi\,. \tag{6.108}$$

The tangent t_1 at the arbitrary point $\psi = \psi_1$ has the normal form

$$x\cos\alpha + y\sin\alpha = p_1\,. \tag{6.109}$$

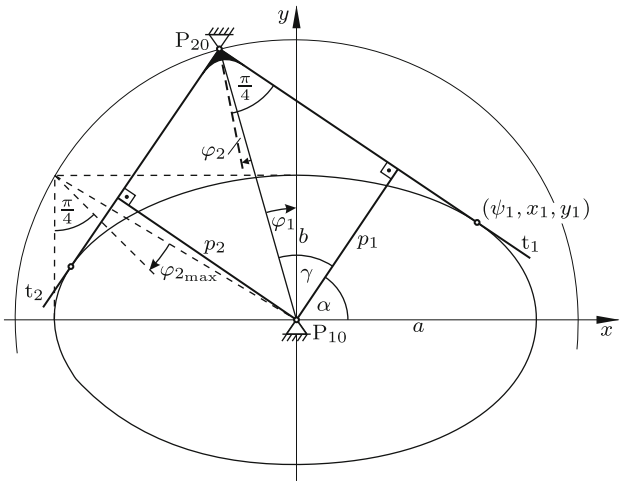

Fig. 6.15 Cam mechanism based on De la Hire's theorem on ellipses

The angle α and the length p_1 of the perpendicular from the origin onto the tangent depend on ψ_1. This dependency is investigated as follows. Through ψ_1 the new angle β is defined by the equations $\cos\psi_1 = (a/p_1)\cos\beta$, $\sin\psi_1 = (b/p_1)\sin\beta$. Together with (6.108) this yields for the coordinates x_1, y_1 associated with ψ_1 the expressions $x_1 = (a^2/p_1)\cos\beta$, $y_1 = (b^2/p_1)\sin\beta$. By assumption, these coordinates satisfy (6.107) as well as (6.109). Substitution yields the equations

$$a^2\cos^2\beta + b^2\sin^2\beta = p_1^2\,, \qquad a^2\cos\beta\cos\alpha + b^2\sin\beta\sin\alpha = p_1^2\,. \quad (6.110)$$

From them it follows that $\beta = \alpha$ and, furthermore,

$$p_1^2 = a^2\cos^2\alpha + b^2\sin^2\alpha = \frac{1}{2}(a^2+b^2) + \frac{1}{2}(a^2-b^2)\cos 2\alpha\,. \quad (6.111)$$

A tangent t_2 orthogonal to t_1 has in its normal form the parameters $\alpha \pm \pi/2$ and p_2. For this tangent (6.111) has the form $p_2^2 = a^2\sin^2\alpha + b^2\cos^2\alpha$. Hence $p_1^2 + p_2^2 = a^2 + b^2$. This concludes the proof.

The angle γ shown in the figure is determined by

$$\cos^2\gamma = \frac{p_1^2}{a^2+b^2} = \frac{1}{2} + \frac{1}{2}\,\frac{a^2-b^2}{a^2+b^2}\cos 2\alpha\,. \quad (6.112)$$

Hence

$$\cos 2\gamma = \frac{a^2-b^2}{a^2+b^2}\cos 2\alpha\,. \quad (6.113)$$

Imagine now that the ellipse is free to rotate about its center P_{10}, and that the right angle formed by t_1 and t_2 is materialized as rigid body with a fixed center at P_{20}. Then the ellipse can rotate full circle. In every position it is in tangential contact with the arms t_1 and t_2. The ellipse represents a cam, and the right angle is the follower driven by the cam. The system is mobile with degree of freedom $F = 1$. Grübler's formula (4.2) with $n = m = 3$ and $f_1 = f_2 = f_3 = 1$ yields $F = d$. This shows that the system is overconstrained with $d = 1$. Manufacturing errors result in the loss of mobility.

As angular coordinate of the cam the angle φ_1 from the frame-fixed line $\overline{P_{10}P_{20}}$ to the minor principal axis of the ellipse is chosen and as coordinate of the follower the angle φ_2 from the same frame-fixed line to the bisector of the right angle (φ_1, φ_2 positive clockwise). The figure shows that $\gamma = \varphi_2 + \pi/4$ and $\gamma - \varphi_1 + \alpha = \pi/2$. Together with (6.113) this yields

$$\varphi_1 = \varphi_2 + \alpha(\varphi_2) - \frac{\pi}{4} \qquad \text{with} \qquad \cos 2\alpha = -\frac{a^2 + b^2}{a^2 - b^2} \sin 2\varphi_2 \,. \tag{6.114}$$

This equation cannot be solved explicitly for φ_2. However, the following statements are obviously true. The angle φ_2 is an odd, π-periodic function of φ_1. It is zero for $\varphi_1 = k\pi/2$ $(k = 0, 1, 2, \cdots)$. Stationary values of φ_2 occur in positions when the principal axes of the ellipse are parallel to t_1 and to t_2 (the dashed lines in Fig. 6.15). The figure yields $\varphi_{2_{\max}} = \tan^{-1}(a/b) - \pi/4$ for $\varphi_1 = \tan^{-1}(a/b)$. Differentiation of both Eqs.(6.114) with respect to time yields the angular velocity ratio

$$\frac{\dot{\varphi}_1}{\dot{\varphi}_2} = 1 + \frac{a^2 + b^2}{a^2 - b^2} \frac{\cos 2\varphi_2}{\sin 2\alpha} \,. \tag{6.115}$$

During the quarter revolution of the ellipse from the position $\varphi_1 = \varphi_2 = 0$, $\alpha = \pi/4$ to the position $\varphi_1 = \pi/2$, $\varphi_2 = 0$, $\alpha = 3\pi/4$ this ratio changes from the extremal value $2a^2/(a^2 - b^2)$ through ∞ at $\varphi_2 = \varphi_{2_{\max}}$ to the extremal value $-2b^2/(a^2 - b^2)$. This investigation is continued in Ex. 1 of Sect. 15.1.2.

6.11 Heureka Octahedron

In Fig. 6.16a a regular octahedron is shown. It has eight faces $1, \ldots, 8$ (equilateral triangles) and six corners. Each corner is common to four faces. At each corner the four faces are grouped in two pairs of adjacent faces. The pairs are identified by the face labels separated by a komma. Examples: At the top corner pairs 1,4 and 2,3 and at the bottom corner pairs 5,8 and 6,7. Imagine the faces to be bodies pairwise interconnected by identical joints at

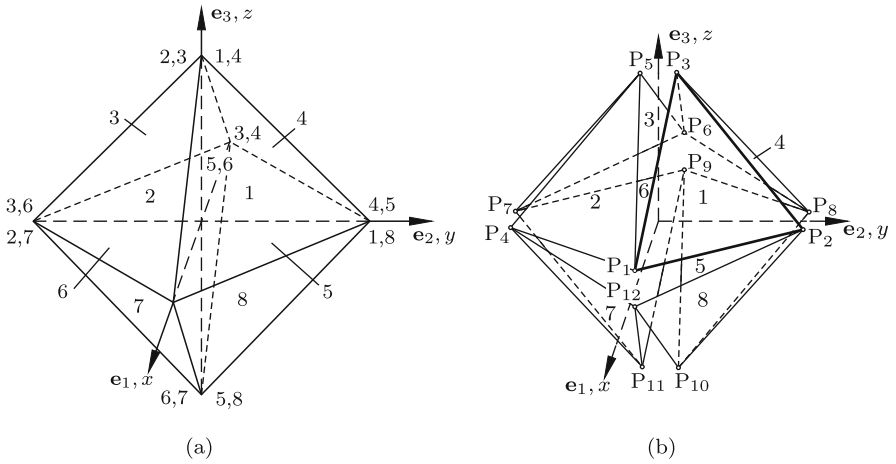

Fig. 6.16 Regular octahedron **(a)** and octahedral mechanism with twelve joints unfolded **(b)**. Front faces 1, 2, 7, 8

the corners (one joint connecting pair 1,4 and another joint connecting pair 2,3 at the top corner etc.). The resulting mechanism has $n = 8$ identical bodies and $m = 12$ identical joints. With f being the individual degree of freedom of a single joint Grübler's Eq.(4.1) yields for the total degree of freedom of the mechanism the formula $F = d + 12f - 30$. This is $F = d + 6$ in the case of spherical joints and $F = d - 6$ in the case of joints with $f = 2$ (universal joints). In Fig. 6.16b a mechanism with spherical joints is shown in a slightly unfolded position which is preserving the original symmetry. The joints are denoted $\mathrm{P}_1, \ldots, \mathrm{P}_{12}$. Example: Face 1 is connected to face 2 by joint P_1, to face 8 by joint P_2 and to face 4 by joint P_3. In what follows, it is shown that the total degree of freedom is $F = 1$ if universal joints are employed provided the two axes of rotation of the joint, each fixed on one of the connected bodies, are properly directed relative to the bodies. In 1991 a very large mechanism of this kind was a major attraction at the Scientific Exhibition HEUREKA at Zurich. Since then the mechanism is known as Heureka octahedron. Since it is $d = 7$ times overconstrained, it became the subject of scientific investigations (Stachel [30], Zsombor Murray [36], Baker [6], Wohlhart [35]). The analysis presented here is different.

The Heureka octahedron is a multiloop mechanism. This is seen from the so-called system graph shown in Fig. 6.17. Its vertices $1, \ldots, 8$ represent the bodies, and its edges $1, \ldots, 12$ (straight or curved lines) represent the joints. The appearance of a graph depends on the labeling of bodies and of joints, on the arrangement of vertices on the sheet of paper and on the shape chosen for the connecting lines. A well-drawn graph should display structural symmetries of the mechanism as clearly as possible. If possible, crossings of edges should be avoided (this is not always possible). The graph in Fig.

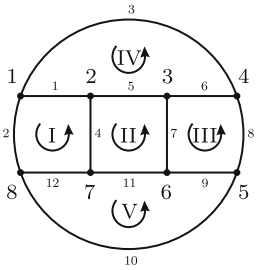

Fig. 6.17 System graph of the Heureka octahedron with elementary loops I – V

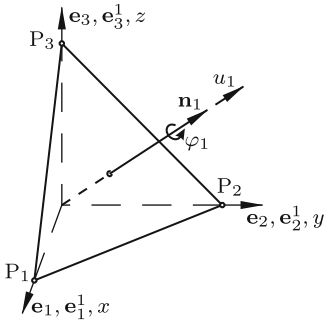

Fig. 6.18 Screw motion of face 1

6.17 is free of crossings and highly symmetric. It reveals the existence of five elementary loops I, II, III, IV and V. Each elementary loop is formed by four bodies and four joints. Other loops present in the graph are combinations of elementary loops. For proving that the Heureka octahedron has the degree of freedom $F = 1$ it suffices to prove that a single independent variable determines the kinematics of all five elementary loops. The proof is achieved as follows. First, the triangular face 1 of Fig. 6.16a is considered when it is isolated from its three neighbors. In Fig. 6.18 it is shown in the fixed reference basis $\underline{\mathbf{e}}$. The outward normal to face 1 is specified by its unit vector $\mathbf{n}_1$ with coordinates $n_1 = n_2 = n_3 = \sqrt{3}/3$. The circular cylinder with axis $\mathbf{n}_1$ which is circumscribing the triangle intersects the $\mathbf{e}_1, \mathbf{e}_2$-plane, the $\mathbf{e}_2, \mathbf{e}_3$-plane and the $\mathbf{e}_3, \mathbf{e}_1$-plane in three congruent ellipses. Clearly, it is possible to subject face 1 to a continuous screw motion with rotation φ_1 about $\mathbf{n}_1$ and with translation $u_1(\varphi_1)$ along $\mathbf{n}_1$ in such a way that P_1 moves along the ellipse in the $\mathbf{e}_3, \mathbf{e}_1$-plane, P_2 along the ellipse in the $\mathbf{e}_1, \mathbf{e}_2$-plane and P_3 along the ellipse in the $\mathbf{e}_2, \mathbf{e}_3$-plane. In what follows, the translatory displacement u_1 as well as the positions of the three points are determined as functions of φ_1. Let the position shown be the null position $\varphi_1 = 0$, $u_1 = 0$. Let, furthermore, $\underline{\mathbf{e}}^1$ be the body-fixed basis which coincides with $\underline{\mathbf{e}}$ in the null position. In $\underline{\mathbf{e}}^1$ P_1, P_2, P_3 have the coordinate matrices $\underline{R}_1^1 = [1\ 0\ 0]^T$, $\underline{R}_2^1 = [0\ 1\ 0]^T$ and $\underline{R}_3^1 = [0\ 0\ 1]^T$, respectively. This definition of unit length implies that the side length of the equilateral triangular faces is $\sqrt{2}$, and that the distance of opposite faces of the octahedron (faces 1 and 6, for example) is $4/\sqrt{3}$. Let $\underline{r}_i = [x_i\ y_i\ z_i]^T$ be the coordinate matrix of P_i $(i = 1, 2, 3)$ in $\underline{\mathbf{e}}$ after the screw displacement. It is calculated from the equation

$$\underline{r}_i = \begin{bmatrix} x_i \\ y_i \\ z_i \end{bmatrix} = \underline{A}^1 \underline{R}_i^1 + u_1 \frac{\sqrt{3}}{3} \begin{bmatrix} 1 \\ 1 \\ 1 \end{bmatrix} \qquad (i = 1, 2, 3) \qquad (6.116)$$

where $\underline{A}^1$ is the matrix in (1.49) with $n_1 = n_2 = n_3 = \sqrt{3}/3$. With the abbreviations $c = \cos\varphi_1$, $s = \sin\varphi_1$

$$\begin{bmatrix} x_i \\ y_i \\ z_i \end{bmatrix} = \frac{1}{3}\left(\begin{bmatrix} 1+2c & 1-c-s\sqrt{3} & 1-c+s\sqrt{3} \\ 1-c+s\sqrt{3} & 1+2c & 1-c-s\sqrt{3} \\ 1-c-s\sqrt{3} & 1-c+s\sqrt{3} & 1+2c \end{bmatrix} \underline{R}_i^1 + u_1\sqrt{3} \begin{bmatrix} 1 \\ 1 \\ 1 \end{bmatrix} \right) \tag{6.117}$$

$(i = 1, 2, 3)$. Each of the conditions $y_1 = z_2 = x_3 = 0$ yields

$$u_1(\varphi_1) = \frac{\sqrt{3}}{3}(\cos\varphi_1 - 1) - \sin\varphi_1 \,. \tag{6.118}$$

When this is substituted back into (6.117), the coordinates of the points are obtained:

$$\left.\begin{aligned} x_3 = y_1 = z_2 = 0 \,, \qquad & x_1 = y_2 = z_3 = \cos\varphi_1 - \frac{\sqrt{3}}{3}\sin\varphi_1 \,, \\ & z_1 = x_2 = y_3 = -\frac{2\sqrt{3}}{3}\sin\varphi_1 \,. \end{aligned}\right\} \tag{6.119}$$

These are parameter equations of the three congruent ellipses. When the position of a single point, for example x_2, y_2, is given, the angle φ_1 is determined from the equations

$$\sin\varphi_1 = -x_2\frac{\sqrt{3}}{2} \,, \qquad \cos\varphi_1 = y_2 - \frac{x_2}{2} \,. \tag{6.120}$$

Substitution into the equation $\sin^2\varphi_1 + \cos^2\varphi_1 = 1$ yields the parameter-free equation of the ellipse

$$x_2^2 + y_2^2 - x_2 y_2 = 1 \,. \tag{6.121}$$

The other two ellipses have the equations $y_3^2 + z_3^2 - y_3 z_3 = 1$ and $z_1^2 + x_1^2 - z_1 x_1 = 1$. In Fig. 6.19 the x_2, y_2-system, the y_3, z_3-system and the z_1, x_1-system are shown in a single diagram. In this diagram the three ellipses appear as a single curve. The principal-axes system ξ, η of the ellipse is rotated 45° against the coordinate axes. In this ξ, η-system the equation of the ellipse is

$$\frac{\xi^2}{2} + \frac{\eta^2}{2/3} = 1 \,. \tag{6.122}$$

The angles $\varphi_1 = -60°$ and $\varphi_1 = 30°$ mark two vertices of the ellipse. The vertices at $\varphi_1 = -60°$ and $\varphi_1 = 120°$ are the points of maximum and minimum translatory displacements $u_{1\max} = \sqrt{3}/3$ and $u_{1\min} = -\sqrt{3}$, respectively. From Fig. 6.16b it is seen that all three coordinates of P_1, P_2, P_3 as well as u_1 must be nonnegative in order to prevent interference of face 1 with other faces. Hence φ_1 is confined to the interval $-120° \le \varphi_1 \le 0$.

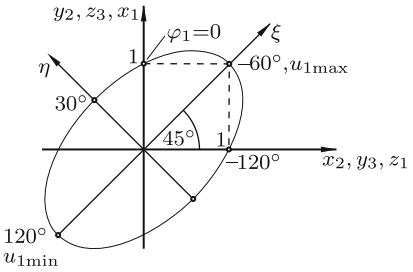

Fig. 6.19 Elliptic trajectories of P_1, P_2, P_3

At $\varphi_1 = -120°$ P_1 (P_2, P_3) is in the position initially held by P_3 (by P_1, by P_2).

Not only the isolated face 1, but every isolated face i $(i = 1, \ldots, 8)$ of the octahedron is able to execute a screw motion φ_i, u_i about its outward normal unit vector $\mathbf{n}_i$ in such a way that each of its three corners moves in one of the principal planes of basis $\underline{\mathbf{e}}$. The position shown in Fig. 6.16a is the null position $\varphi_i = 0$ $(i = 1, \ldots, 8)$. Independent of which face is chosen the three coordinates of $\mathbf{n}_i$ have identical absolute values $\sqrt{3}/3$. From this it follows that, independent of the choice of face, the circular cylinder which has $\mathbf{n}_i$ as axis and which circumscribes the triangle of face i intersects the principal planes of basis $\underline{\mathbf{e}}$ in the same three ellipses. For each of the faces $2, \ldots, 8$ the analysis differs from the one for face 1 in the signs of certain vector coordinates. In what follows, these changes are shown for face 2. The unit normal vector $\mathbf{n}_2$ has coordinates $\sqrt{3}/3[1 \;\; -1 \;\; 1]^T$. The minus sign has the effect that the transformation matrix relating bases $\underline{\mathbf{e}}$ and $\underline{\mathbf{e}}^2$ (fixed on face 2 and coinciding with $\underline{\mathbf{e}}$ in the position $\varphi_2 = 0$) is with new abbreviations $c = \cos\varphi_2$, $s = \sin\varphi_2$

$$\underline{A}^2 = \frac{1}{3}\begin{bmatrix} 1+2c & -(1-c)-s\sqrt{3} & 1-c-s\sqrt{3} \\ -(1-c)+s\sqrt{3} & 1+2c & -(1-c)-s\sqrt{3} \\ 1-c+s\sqrt{3} & -(1-c)+s\sqrt{3} & 1+2c \end{bmatrix} . \quad (6.123)$$

In basis $\underline{\mathbf{e}}^2$ P_1, P_4, P_5 have the coordinate matrices $\underline{R}_1^2 = [1 \;\; 0 \;\; 0]^T$, $\underline{R}_4^2 = [0 \;\; -1 \;\; 0]^T$ and $\underline{R}_5^2 = [0 \;\; 0 \;\; 1]^T$, respectively. In the analysis of face 1 it has already been decided that P_1 moves along the ellipse in the $\mathbf{e}_3, \mathbf{e}_1$-plane. Face 2 is connected to face 1 at P_1. The previously specified motion of P_1 in the $\mathbf{e}_3, \mathbf{e}_1$-plane is compatible with screw motion about $\mathbf{n}_2$ only if P_4 moves along the ellipse in the $\mathbf{e}_1, \mathbf{e}_2$-plane and P_5 along the ellipse in the $\mathbf{e}_2, \mathbf{e}_3$-plane. These are the only differences as compared with face 1. The same calculations which led to (6.118) and (6.119) now lead to

$$u_2(\varphi_2) = \frac{\sqrt{3}}{3}(\cos\varphi_2 - 1) + \sin\varphi_2 , \quad (6.124)$$

$$\left.\begin{aligned} y_1 = z_4 = x_5 = 0\ , \qquad & x_1 = -y_4 = z_5 = \cos\varphi_2 + \frac{\sqrt{3}}{3}\sin\varphi_2\ , \\ & z_1 = x_4 = -y_5 = \frac{2\sqrt{3}}{3}\sin\varphi_2\ . \end{aligned}\right\} \tag{6.125}$$

Face 7 is connected to face 2 at P_4. The previously specified motion of P_4 in the $\mathbf{e}_1, \mathbf{e}_2$-plane is compatible with screw motion about $\mathbf{n}_7$ only if P_{11} moves in the $\mathbf{e}_2, \mathbf{e}_3$-plane and P_{12} in the $\mathbf{e}_3, \mathbf{e}_1$-plane. The equations equivalent to (6.118) and (6.119) are

$$u_7(\varphi_7) = \frac{\sqrt{3}}{3}(\cos\varphi_7 - 1) - \sin\varphi_7\ , \tag{6.126}$$

$$\left.\begin{aligned} y_{12} = z_4 = x_{11} = 0\ , \quad & x_{12} = -y_4 = -z_{11} = \cos\varphi_7 - \frac{\sqrt{3}}{3}\sin\varphi_7\ , \\ & z_{12} = -x_4 = y_{11} = \frac{2\sqrt{3}}{3}\sin\varphi_7\ . \end{aligned}\right\} \tag{6.127}$$

Face 6 is connected to face 7 at P_{11}. The previously specified motion of P_{11} in the $\mathbf{e}_2, \mathbf{e}_3$-plane is compatible with screw motion about $\mathbf{n}_6$ only if P_9 moves in the $\mathbf{e}_3, \mathbf{e}_1$-plane and P_7 in the $\mathbf{e}_1, \mathbf{e}_2$-plane. The equations equivalent to (6.118) and (6.119) are

$$u_6(\varphi_6) = \frac{\sqrt{3}}{3}(\cos\varphi_6 - 1) + \sin\varphi_6\ , \tag{6.128}$$

$$\left.\begin{aligned} x_{11} = y_9 = z_7 = 0\ , \qquad & z_{11} = x_9 = y_7 = -\cos\varphi_6 - \frac{\sqrt{3}}{3}\sin\varphi_6\ , \\ & y_{11} = z_9 = x_7 = -\frac{2\sqrt{3}}{3}\sin\varphi_6\ . \end{aligned}\right\} \tag{6.129}$$

Face 8 is connected to face 7 at P_{12}. For this reason P_{12} is required to move in the $\mathbf{e}_3, \mathbf{e}_1$-plane. At this point it is not yet required that the loop I formed by faces 1, 2, 7 and 8 be closed at P_2. Let P_2^* be the point fixed on face 8 which coincides with P_2. The prescribed motion of P_{12} is compatible with screw motion about $\mathbf{n}_8$ only if P_2^* moves in the $\mathbf{e}_1, \mathbf{e}_2$-plane and P_{10} in the $\mathbf{e}_2, \mathbf{e}_3$-plane. The equations equivalent to (6.118) and (6.119) are

$$u_8(\varphi_8) = \frac{\sqrt{3}}{3}(\cos\varphi_8 - 1) + \sin\varphi_8\ , \tag{6.130}$$

$$\left.\begin{aligned} z_2^* = x_{10} = y_{12} = 0\ , \quad & y_2^* = -z_{10} = x_{12} = \cos\varphi_8 + \frac{\sqrt{3}}{3}\sin\varphi_8\ , \\ & x_2^* = y_{10} = -z_{12} = \frac{2\sqrt{3}}{3}\sin\varphi_8\ . \end{aligned}\right\} \tag{6.131}$$

Closure of loop I at P_2 requires that $x_2^* \equiv x_2$ and $y_2^* \equiv y_2$. This is, indeed, the case. Equations (6.131), (6.127), (6.125) and (6.119) yield $x_2^* = -z_{12} = x_4 = z_1 \equiv x_2$ and $y_2^* = x_{12} = -y_4 = x_1 \equiv y_2$.

The closure of the other four elementary loops is proved in the same way by subjecting faces 3, 4 and 5 to screw displacements about their outward normals. For reasons of symmetry this is unnecessary. Each loop is composed of four faces and four joints. In the folded position of the mechanism shown in Fig. 6.16a two of the four joints coincide in one corner of the octahedron. In loop I joints P_1 and P_{12} coincide at the front corner with coordinates $(x, y, z) = (1\ 0\ 0)$. In loop II joints P_4 and P_7 coincide at the corner $(0\ -1\ 0)$. In loop III joints P_6 and P_9 coincide at the corner $(-1\ 0\ 0)$. In loop IV joints P_3 and P_5 coincide at the top corner $(0\ 0\ 1)$, and in loop V joints P_{10} and P_{11} coincide at the bottom corner $(0\ 0\ -1)$. In every loop the geometry is the same.

Equations (6.125) and (6.119) express x_1 and z_1 once in terms of φ_1 and once in terms of φ_2. The pairwise identity of the two expressions has the form

$$\cos\varphi_2 + \frac{\sqrt{3}}{3}\sin\varphi_2 \equiv \cos\varphi_1 - \frac{\sqrt{3}}{3}\sin\varphi_1\ , \qquad \frac{2\sqrt{3}}{3}\sin\varphi_2 \equiv -\frac{2\sqrt{3}}{3}\sin\varphi_1\ . \tag{6.132}$$

Hence $\varphi_2 \equiv -\varphi_1$. Also for the coordinates of P_4, P_{11} and P_{12} two expressions in terms of two angles have been formulated. They lead to the identities $\varphi_7 \equiv -\varphi_2 \equiv \varphi_1$, $\varphi_6 \equiv -\varphi_7 \equiv \varphi_1$ and $\varphi_8 \equiv -\varphi_7 \equiv \varphi_1$. The general rule is that screw angles of any two faces coupled by a joint are of equal magnitude and opposite sign:

$$\varphi_3 \equiv \varphi_5 \equiv \varphi_7 \equiv \varphi_1\ , \qquad \varphi_2 \equiv \varphi_4 \equiv \varphi_6 \equiv \varphi_8 \equiv -\varphi_1\ . \tag{6.133}$$

These equations in combination with (6.118), (6.124), (6.126), (6.128) and (6.130) prove that all translatory displacements are identical (either all of them outward or all inward):

$$u_i(\varphi_1) \equiv u(\varphi_1) = \frac{\sqrt{3}}{3}(\cos\varphi_1 - 1) - \sin\varphi_1 \qquad (i = 1, \ldots, 8)\ . \tag{6.134}$$

Opposite faces of the octahedron have identical products screw angle times unit normal vector ($\varphi_6\mathbf{n}_6 = \varphi_1\mathbf{n}_1$, for example). From this it follows that the motion of opposite faces relative to each other is pure translation $2u(\varphi_1)$ along the common normal. For faces 1 and 6 this follows also from (6.129), (6.127), (6.125) and (6.119). In combination they state that the coordinates of opposite joints of the two faces (joints P_1 and P_9, joints P_2 and P_7, joints P_3 and P_{11}) are of equal magnitude and opposite sign: $x_9 = -x_1$, $y_9 = -y_1$, $z_9 = -z_1$ etc. In Fig. 6.16b this is shown.

Through the same Eqs.(6.129), (6.127), (6.125) and (6.119) the coordinates of all twelve points P_i $(i = 1, \ldots, 12)$ are expressed in terms of the coordi-

nates x_1 and z_1 of P_1. The coordinates are collected in Table 6.1. Column i of this table $(i = 1, \ldots, 12)$ is the coordinate matrix $\underline{r}_i = [x_i \; y_i \; z_i]^T$.

Table 6.1 Coordinates x_i, y_i, z_i of points P_i $(i = 1, \ldots, 12)$ in basis $\underline{\mathbf{e}}$

	1	2	3	4	5	6	7	8	9	10	11	12
x_i	x_1	z_1	0	z_1	0	$-x_1$	$-z_1$	$-z_1$	$-x_1$	0	0	x_1
y_i	0	x_1	z_1	$-x_1$	$-z_1$	0	$-x_1$	x_1	0	z_1	$-z_1$	0
z_i	z_1	0	x_1	0	x_1	z_1	0	0	$-z_1$	$-x_1$	$-x_1$	$-z_1$

$$x_1 = \cos\varphi_1 - \frac{\sqrt{3}}{3}\sin\varphi_1 \,, \qquad z_1 = -\frac{2\sqrt{3}}{3}\sin\varphi_1 \,.$$

At both ends of the admissible interval $-120^\circ \le \varphi_1 \le 0$ the eight faces form a closed octahedron. At $\varphi_1 = -60^\circ$ the eight faces experience the maximum outward translatory displacement $u_{\max} = \sqrt{3}/3$.

The motion of the mechanism described above is possible with twelve spherical joints. What remains to be shown is that it is possible with two-degree-of-freedom joints as well. This is done as follows. For reasons of symmetry it suffices to consider faces 1 and 2 coupled by joint P_1. Let $\boldsymbol{\Omega}_{21}$ be the angular velocity of face 2 relative to face 1 about the common point P_1. It is the difference $\boldsymbol{\Omega}_{21} = \boldsymbol{\omega}_2 - \boldsymbol{\omega}_1$ of the angular velocities of faces 2 and 1, respectively, relative to basis $\underline{\mathbf{e}}$. This difference is $\boldsymbol{\Omega}_{21} = \dot{\varphi}_2\mathbf{n}_2 - \dot{\varphi}_1\mathbf{n}_1 = -\dot{\varphi}_1(\mathbf{n}_2 + \mathbf{n}_1)$. The vectors $\mathbf{n}_1$ and $\mathbf{n}_2$ are fixed in basis $\underline{\mathbf{e}}$. The constant angle α between them is determined by $\cos\alpha = \mathbf{n}_1 \cdot \mathbf{n}_2$. The coordinates $(\sqrt{3}/3)[1 \;\; 1 \;\; 1]$ of $\mathbf{n}_1$ and $(\sqrt{3}/3)[1 \;\; -1 \;\; 1]$ of $\mathbf{n}_2$ determine $\cos\alpha = 1/3$ $(\alpha \approx 70.5^\circ)$. The vector $\mathbf{n}_2 + \mathbf{n}_1$ and, therefore, also $\boldsymbol{\Omega}_{21}$ is directed along the bisector of this angle. Hence the joint connecting faces 1 and 2 is a two-degree-of-freedom joint with an axis of rotation 1 fixed on face 1 in the direction of $\mathbf{n}_1$ and with an axis of rotation 2 fixed on face 2 in the direction of $\mathbf{n}_2$ (see Fig. 6.20). This joint is a universal joint with nonorthogonal axes intersecting at P_1.

Faces 7 and 6 are separated from face 1 by two and by three joints, respectively. Let $\boldsymbol{\Omega}_{71}$ and $\boldsymbol{\Omega}_{61}$ be their angular velocities relative to face 1. These angular velocities are $\boldsymbol{\Omega}_{71} = \dot{\varphi}_7\mathbf{n}_7 - \dot{\varphi}_1\mathbf{n}_1 = \dot{\varphi}_1(\mathbf{n}_7 - \mathbf{n}_1)$ and $\boldsymbol{\Omega}_{61} = \dot{\varphi}_6\mathbf{n}_6 - \dot{\varphi}_1\mathbf{n}_1 \equiv \mathbf{0}$. The latter formula reconfirms that face 6 is in pure translation relative to face 1. The former can be written in the alternative forms $\boldsymbol{\Omega}_{71} = \dot{\varphi}_1(\mathbf{n}_7 + \mathbf{n}_6) = \boldsymbol{\Omega}_{76}$ and $\boldsymbol{\Omega}_{71} = -\dot{\varphi}_1(\mathbf{n}_4 + \mathbf{n}_1) = -\boldsymbol{\Omega}_{41}$. These equations show that the relative angular velocities of all pairs of nonopposite faces have identical absolute values.

The Heureka octahedron at the Scientific Exhibition at Zurich would not have been a major attraction had only the identical screw motions of the eight faces relative to basis $\underline{\mathbf{e}}$ been demonstrated. Since one face of the octahedron was fixed horizontally to the ground, not the motion relative to basis $\underline{\mathbf{e}}$ was visible, but the motion of the remaining seven faces relative to the fixed face.

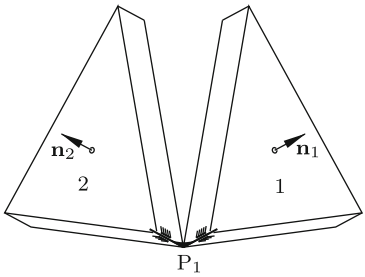

Fig. 6.20 Universal joint with nonorthogonal axes

Viewers were allowed to stand on this face while the octahedron was opening and closing around them. In what follows, it is assumed that face 1 is fixed. To be determined are the trajectories, i.e., the coordinate matrices of the points P_i $(i = 1, \ldots, 12)$ in basis $\underline{\mathbf{e}}^1$ as functions of φ_1. These matrices are denoted $\underline{R}_i^1 = [X_i\ Y_i\ Z_i]^T$. Inversion of (6.116) yields the explicit formula

$$\underline{R}_i^1 = \begin{bmatrix} X_i \\ Y_i \\ Z_i \end{bmatrix} = \underline{A}^{1\,T} \underline{r}_i - u \frac{\sqrt{3}}{3} \begin{bmatrix} 1 \\ 1 \\ 1 \end{bmatrix} \qquad (i = 1, \ldots, 12) \tag{6.135}$$

or with the abbreviations $c = \cos\varphi_1$, $s = \sin\varphi_1$ and with u from (6.134)

$$\begin{bmatrix} X_i \\ Y_i \\ Z_i \end{bmatrix} = \frac{1}{3} \left(\begin{bmatrix} 1+2c & 1-c+s\sqrt{3} & 1-c-s\sqrt{3} \\ 1-c-s\sqrt{3} & 1+2c & 1-c+s\sqrt{3} \\ 1-c+s\sqrt{3} & 1-c-s\sqrt{3} & 1+2c \end{bmatrix} \underline{r}_i + (1-c+s\sqrt{3}) \begin{bmatrix} 1 \\ 1 \\ 1 \end{bmatrix} \right) \tag{6.136}$$

$(i = 1, \ldots, 12)$. The coordinate matrices $\underline{r}_i$ in basis $\underline{\mathbf{e}}$ are known from Table 6.1. Evaluation for $i = 1, 4, 5, 7, 9, 11$ and 12 yields as functions of φ_1 the coordinates of the points fixed on faces 2, 6 and 7:

$$\left.\begin{aligned} X_1 &= 1\,, & X_4 &= \frac{2}{3}\left[s(1-4c)\frac{\sqrt{3}}{3} - c + 1\right], & X_5 &= \frac{4\sqrt{3}}{9}\, s(1-c+s\sqrt{3})\,, \\ Y_1 &= 0\,, & Y_4 &= \frac{2}{3}\left[s(1+2c)\frac{\sqrt{3}}{3} - c - 2c^2\right] + 1\,, & Y_5 &= \frac{4\sqrt{3}}{9}\, s(1+2c)\,, \\ Z_1 &= 0\,, & Z_4 &= \frac{2}{3}\left[s(1+2c)\frac{\sqrt{3}}{3} - c + 2c^2 - 1\right], & Z_5 &= \frac{4\sqrt{3}}{9}\, s(1-c-s\sqrt{3}) + 1\,, \end{aligned}\right\} \tag{6.137}$$

$$\left.\begin{aligned} X_{11} &= -\frac{2\sqrt{3}}{3}\, u\,, & X_7 &= X_{11}\,, & X_9 &= X_{11} - 1\,, & X_{12} &= Z_5\,, \\ Y_{11} &= X_{11}\,, & Y_7 &= X_{11} - 1\,, & Y_9 &= X_{11}\,, & Y_{12} &= X_5\,, \\ Z_{11} &= X_{11} - 1\,, & Z_7 &= X_{11}\,, & Z_9 &= X_{11}\,, & Z_{12} &= Y_5\,. \end{aligned}\right\} \tag{6.138}$$

Differentiation of the coordinates with respect to time yields the velocities of the points. The velocities of P_4 and P_5 are $v_4 = \frac{4}{3}\dot{\varphi}_1\sqrt{2 + (c + s\sqrt{3})^2/4} = \frac{4}{3}\dot{\varphi}_1\sqrt{2 + \cos^2(\varphi_1 - 60°)}$, $v_5 = \frac{4}{3}\dot{\varphi}_1\sqrt{2 + \cos^2\varphi_1}$.

P_4 and P_5 are both located on the sphere of radius $\sqrt{2}$ centered at P_1. Hence $(X_4-1)^2+Y_4^2+Z_4^2=2$ and $(X_5-1)^2+Y_5^2+Z_5^2=2$.
P_4 as well as P_5 is located on still another second-order surface. By substituting coordinates it is verified that

$$Y_4-Z_4+1=\tfrac{8}{3}s^2\,,\qquad Y_4+Z_4-2X_4+1=\tfrac{8}{3}\sqrt{3}\,sc\,,$$
$$X_5-Z_5+1=\tfrac{8}{3}s^2\,,\qquad X_5+Y_5+Z_5-1=\tfrac{4}{3}\sqrt{3}\,s\,.$$

Hence

$$(Y_4+Z_4-2X_4+1)^2-(1+Y_4-Z_4)[5-3(Y_4-Z_4)]=0$$

or
$$[\,X_4\;Y_4\;Z_4\,]\begin{bmatrix}2&-1&-1\\-1&2&-1\\-1&-1&2\end{bmatrix}\begin{bmatrix}X_4\\Y_4\\Z_4\end{bmatrix}-2X_4+2Z_4-2=0$$

and

$$(X_5+Y_5+Z_5-1)^2-2(X_5-Z_5+1)=0$$

or
$$[\,X_5\;Y_5\;Z_5\,]\begin{bmatrix}1&1&1\\1&1&1\\1&1&1\end{bmatrix}\begin{bmatrix}X_5\\Y_5\\Z_5\end{bmatrix}-4X_5-2Y_5-1=0\,.$$

In both equations the symmetric coefficient matrix of the second-order terms has real eigenvalues λ_1, λ_2, λ_3 and mutually orthogonal eigenvectors. Let $\underline{A}_i$ $(i=4,5)$ be the matrix with these eigenvectors as columns. The transformation $[\,X_i\;Y_i\;Z_i\,]^T=\underline{A}_i\,[\,x\;y\;z\,]^T$ results in an equation of the form $\lambda_1x^2+\lambda_2y^2+\lambda_3z^2+ax+by+cz+d=0$.

The equation for P_4:
$\lambda_1=0$, $\lambda_2=\lambda_3=3$, $\underline{A}_4=\frac{1}{6}\begin{bmatrix}2\sqrt{3}&3\sqrt{2}&\sqrt{6}\\2\sqrt{3}&-3\sqrt{2}&\sqrt{6}\\2\sqrt{3}&0&-2\sqrt{6}\end{bmatrix}$. The transformed equation is $(y-\frac{1}{6}\sqrt{2})^2+(z-\frac{1}{6}\sqrt{6})^2=\frac{8}{9}$. This is a circular cylinder. Its radius is twice the radius of the circle circumscribing the triangular face of the octahedron.

The equation for P_5:
$\lambda_1=3$, $\lambda_2=\lambda_3=0$, $\underline{A}_5=\frac{1}{6}\begin{bmatrix}-2\sqrt{3}&\sqrt{6}&-3\sqrt{2}\\-2\sqrt{3}&-2\sqrt{6}&0\\-2\sqrt{3}&\sqrt{6}&3\sqrt{2}\end{bmatrix}$. The transformed equation is $(x\sqrt{3}+1)^2+2z\sqrt{2}-2=0$. This is a cylinder with parabolic cross section in the x,z-plane.

Generalized Heureka Octahedron

The triangle shown in Fig. 6.21 in basis $\underline{\mathbf{e}}$ has its corners at points with coordinate matrices $\underline{R}_1^1=[a_1\;0\;0]^T$, $\underline{R}_2^1=[0\;a_2\;0]^T$ and $\underline{R}_3^1=[0\;0\;a_3]^T$, respectively ($a_1$, a_2, $a_3>0$ arbitrary). This triangle is face 1 of a plane-symmetric octahedron with these corners and with the opposite corners $-\underline{R}_1^1$, $-\underline{R}_2^1$ and $-\underline{R}_3^1$. The labeling of faces, the pairwise connections of faces by joints and the labeling of joints are copied from Figs. 6.16a and b. Proposition: If the joint at P_i $(i=1,\ldots,12)$ is a universal joint with joint axes along the normals of the two bodies coupled by this joint, the mechanism has the degree of freedom $F=1$. Furthermore, each face $i=1,\ldots,8$ moves in such

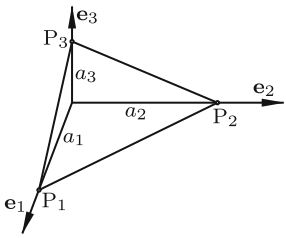

Fig. 6.21 Face 1 of a plane-symmetric octahedron

a way that (i) its normal $\mathbf{n}_i$ does not change its direction and (ii) each corner moves in an ellipse in a principle plane of basis $\underline{\mathbf{e}}$. The idea to generalize the Heureka octahedron in this way is due to Wohlhart [34]. The proof presented here is different.

For reasons of symmetry it suffices to prove the propositions for face 1. Its outward normal unit vector has the coordinates (normalized vector product $\overrightarrow{\mathrm{P_1P_2}} \times \overrightarrow{\mathrm{P_1P_3}}$)

$$n_1 = \frac{a_2 a_3}{N} \ , \quad n_2 = \frac{a_3 a_1}{N} \ , \quad n_3 = \frac{a_1 a_2}{N} \ , \quad N = \sqrt{a_1^2 a_2^2 + a_2^2 a_3^2 + a_3^2 a_1^2} \ . \tag{6.139}$$

From the analysis of the Heureka octahedron the conditions are copied that $\mathrm{P_1}$ moves in the $\mathbf{e}_3, \mathbf{e}_1$-plane, $\mathrm{P_2}$ in the $\mathbf{e}_1, \mathbf{e}_2$-plane and $\mathrm{P_3}$ in the $\mathbf{e}_2, \mathbf{e}_3$-plane. These conditions plus the stationarity condition of the unit normal vector require that the displacement of face 1 is a rotation about the unit normal vector superimposed by a translation which does not have the direction of the unit normal vector. Equation (6.116) is replaced by the equation

$$\begin{bmatrix} x_i \\ y_i \\ z_i \end{bmatrix} = \underline{A}^1 \underline{R}_i^1 + \begin{bmatrix} u_1 \\ u_2 \\ u_3 \end{bmatrix} \qquad (i = 1, 2, 3) \ , \tag{6.140}$$

where u_1, u_2, u_3 are the coordinates of the displacement in basis $\underline{\mathbf{e}}$. With the general Eq.(1.49) for $\underline{A}^1$ this equation is ($c = \cos\varphi_1$, $s = \sin\varphi_1$)

$$\begin{bmatrix} x_i \\ y_i \\ z_i \end{bmatrix} = \begin{bmatrix} n_1^2 + (1 - n_1^2)c & n_1 n_2 (1 - c) - n_3 s & n_1 n_3 (1 - c) + n_2 s \\ n_1 n_2 (1 - c) + n_3 s & n_2^2 + (1 - n_2^2)c & n_2 n_3 (1 - c) - n_1 s \\ n_1 n_3 (1 - c) - n_2 s & n_2 n_3 (1 - c) + n_1 s & n_3^2 + (1 - n_3^2)c \end{bmatrix} \underline{R}_i^1 + \begin{bmatrix} u_1 \\ u_2 \\ u_3 \end{bmatrix} \tag{6.141}$$

($i = 1, 2, 3$). For n_1, n_2, n_3 the expressions (6.139) are substituted. The conditions $y_1 = z_2 = x_3 = 0$ yield for the translatory displacements the explicit functions of φ_1:

$$\left.\begin{aligned} u_1 &= -a_3^2 a_1 \Big[\frac{a_2^2}{N^2}(1-\cos\varphi_1) + \frac{1}{N}\,\sin\varphi_1 \Big] \,, \\ u_2 &= -a_1^2 a_2 \Big[\frac{a_3^2}{N^2}(1-\cos\varphi_1) + \frac{1}{N}\,\sin\varphi_1 \Big] \,, \\ u_3 &= -a_2^2 a_3 \Big[\frac{a_1^2}{N^2}(1-\cos\varphi_1) + \frac{1}{N}\,\sin\varphi_1 \Big] \,. \end{aligned}\right\} \tag{6.142}$$

When these expressions are substituted back into (6.141), the coordinates of $\mathrm{P}_1\,,\,\mathrm{P}_2\,,\,\mathrm{P}_3$ in basis $\underline{\mathbf{e}}$ are obtained:

$$\left.\begin{aligned} x_1 &= a_1\Big(\cos\varphi_1 - \frac{a_3^2}{N}\,\sin\varphi_1 \Big) \,, \qquad & z_1 &= -\frac{a_3(a_1^2+a_2^2)}{N}\,\sin\varphi_1 \,, \\ y_2 &= a_2\Big(\cos\varphi_1 - \frac{a_1^2}{N}\,\sin\varphi_1 \Big) \,, \qquad & x_2 &= -\frac{a_1(a_2^2+a_3^2)}{N}\,\sin\varphi_1 \,, \\ z_3 &= a_3\Big(\cos\varphi_1 - \frac{a_2^2}{N}\,\sin\varphi_1 \Big) \,, \qquad & y_3 &= -\frac{a_2(a_3^2+a_1^2)}{N}\,\sin\varphi_1 \,. \end{aligned}\right\} \tag{6.143}$$

Elimination of φ_1 from the equations for x_2 and y_2 proves that the trajectory of P_2 is the ellipse

$$x_2^2\,\frac{(a_1^2+a_2^2)(a_1^2+a_3^2)}{a_1^2(a_2^2+a_3^2)^2} + \frac{y_2^2}{a_2^2} - \frac{2a_1}{a_2(a_2^2+a_3^2)}\,x_2 y_2 = 1 \,. \tag{6.144}$$

The other two ellipses are obtained by cyclic permutation of indices. In the special case $a_1 = a_2 = a_3 = 1$, which characterizes the Heureka octahedron, (6.142) – (6.144) are identical with (6.118), (6.119) and (6.121), respectively. This ends the proof that face 1 is moving in the predicted way. For reasons of symmetry the trajectories of the corners of faces $2,\ldots,8$ are congruent ellipses. For the same reason, also Eqs.(6.133) are valid: $\varphi_3 \equiv \varphi_5 \equiv \varphi_7 \equiv \varphi_1$, $\varphi_2 \equiv \varphi_4 \equiv \varphi_6 \equiv \varphi_8 \equiv -\varphi_1$. In joint P_i $(i = 1,\ldots,12)$ the relative angular velocity of the two coupled faces lies in the plane of the normals of these faces. From this it follows that joint i is a universal joint with joint axes along the normals of the two faces. The cosine of the constant angle α_i between the normals is the scalar product of the unit normal vectors. Face 1 is connected to face 2 by joint 1 (angle α_1), to face 8 by joint 2 (angle α_2) and to face 4 by joint 3 (angle α_3). The same three angles appear in the joints of each face. The four unit normal vectors involved have in basis $\underline{\mathbf{e}}$ the following coordinates: Face 1: $[n_1\ n_2\ n_3]$, face 2: $[n_1\ -n_2\ n_3]$, face 8: $[n_1\ n_2\ -n_3]$, face 4: $[-n_1\ n_2\ n_3]$. With (6.139) this yields

$$\left.\begin{aligned} \cos\alpha_1 &= \frac{a_2^2a_3^2 - a_3^2a_1^2 + a_1^2a_2^2}{a_2^2a_3^2 + a_3^2a_1^2 + a_1^2a_2^2} \,, \qquad & \cos\alpha_2 &= \frac{a_2^2a_3^2 + a_3^2a_1^2 - a_1^2a_2^2}{a_2^2a_3^2 + a_3^2a_1^2 + a_1^2a_2^2} \,, \\ \cos\alpha_3 &= \frac{-a_2^2a_3^2 + a_3^2a_1^2 + a_1^2a_2^2}{a_2^2a_3^2 + a_3^2a_1^2 + a_1^2a_2^2} \,, \qquad & \sum_i \cos\alpha_i &= 1 \,. \end{aligned}\right\} \tag{6.145}$$

References

1. Altmann F G (1954) Räumliche fünfgliedrige Koppelgetriebe. Konstruktion 6:254–259
2. Altmann F G (1954) Über räumliche sechsgliedrige Koppelgetriebe. Z. VDI 96:245–249
3. Baker J E (1979) The Bennett, Goldberg and Myard linkages-in perspective. Mechanism Machine Theory 14:239–253
4. Baker J E (1980) An analysis of the Bricard linkages. Mechanism Machine Theory 15:267–286
5. Baker J E (1984) On 5-revolute linkages with parallel adjacent joint axes. Mechanism Machine Theory 19:467–475
6. Baker J E (1993) On a network of continuously modified Bennett linkages. Proc. 6th Int.Symp. Teoria si Practica Mecanismelor, Bucharesti 2:27–34
7. Baker J E (1993) A comparative survey of the Bennett-based, 6-R revolute kinematic loops. Mechanism Machine Theory 28:83–96
8. Bennett G T (1903) A new mechanism. Engineering 76:77–78
9. Borel E (1908) Mémoire sur les déplacements a trajectoires sphériques. Mém. présenté par divers savants. Paris 2, v.33,1:1–128
10. Bricard R (1926/27) Leçons de cinématique. v.I.: Cinématique théorique. v.II: Cinématique appliquée. Gauthier-Villars, Paris
11. Bricard R (1906) Mémoire sur les déplacements à trajectoires sphériques. J. Ec. Polyt. 2, v.11:1–96
12. Bronstein I N, Semendjajev K A, Musiol K A, Mühlig H (2008) Taschenbuch der Mathematik. 7. Aufl. Verlag Harri Deutsch
13. Byshgens S S (1939) The Bennett-Berkovski mechanism (Russ). PMM v.II:513–518
14. Connelly R (1979) The rigidity of polyhedral surfaces. Mathematics Mag.52:275–283
15. Delassus E (1900) Sur les systèmes articulés gauches. Première Partie. Paris Ec.Normale Sup., Ann.Scie. 3s,XVII:445–499
16. Delassus E (1902) Sur les systèmes articulés gauches. Deuxième Partie. Paris Ec.Normale Sup., Ann.Scie. 3s,XIX:119–152
17. Demaine E D , O'Rourke J (2007) Geometric folding algorithms. Linkages, origami, polyhedra. Cambridge Univ. Press
18. Dimentberg F M, Schor Ja B (1940) The Bennett mechanism. PMM v.IV:111–118
19. Dietmaier P (1995) Einfach übergeschlossene Mechanismen mit Drehgelenken. Habil.-Schrift Graz
20. Goldberg M (1943) New five-bar and six-bar linkages in three dimensions. Trans. ASME 65:649–661
21. Hilbert D, Cohn-Vossen S (1996) Anschauliche Geometrie. 2.Aufl. Springer, Berlin. Engl. trans. (1952) Geometry and the imagination. Chelsea, New York
22. Hon-Cheung Y (1994) published in: Baker E, Wohlhart K: On the single screw reciprocal to the general line-symmetric six-screw linkage. Mechanism Machine Theory 29:169–175
23. Husty M L, Zsombor-Murray P (1994) A special type of singular Stewart–Gough platform. In: [24] 449–458
24. Lenarčič J, Ravani B (eds) (1994) Advances in robot kinematics and computational geometry. Kluwer, Dordrecht
25. Mavroidis C, Roth B (1994) Analysis and synthesis of overconstrained mechanisms. Proc. of 1994 ASME Design Techn. Conf., DE-70, Minneapolis, 115–133
26. Mavroidis C, Roth B (1995) Analysis and synthesis of overconstrained mechanisms. J. Mechanical Design 117:69–74
27. Mavroidis C, Roth B (1995) New and revised overconstrained mechanisms. J. Mechanical Design 117:75–82
28. Mavroidis C, Beddows M (1997) A spatial overconstrained mechanism that can be used in practical applications. Proc. Fifth Appl.Mechanisms

29. Mudrov P G (1976) Spatial mechanisms with revolute joints (Russ.) Isd. Kazan Univ.
30. Stachel H (1992) Zwei bemerkenswerte bewegliche Strukturen. J. Geometry 43:14–21
31. Wohlhart K (1987) A new 6R space mechanism. Proc. 7th IFToMM World Congr. 1:193–198
32. Wohlhart K (1991) Merging two general Goldberg 5R linkages to obtain a new 6R space mechanism. Mechanism Machine Theory 26:659–668
33. Wohlhart K (1993) The two types of orthogonal Bricard mechanism. Mechanism Machine Theory 28:809–817
34. Wohlhart K (1995) Das dreifach plansymmetrische Oktoid und seine Punktbahnen. Mathematica Pannonica 6:243–265
35. Wohlhart K (1995) Heureka Octahedron and Brussels folding cube as special cases of the turing tower. Proc. 6th Int.Symp. Teoria si Practica Mecanismelor, Bucharesti 2:302–311
36. Zsombor Murray P J (1992) The Brussels folding cube. Proc.3rd Int.Workshop Advances in Robot Kinematics:159–164